Analysis and Design of Wireless Two-Way Relay Networks with Energy Harvesting

M.Tech. Thesis

By

UGRASEN SINGH

DISCIPLINE OF ELECTRICAL ENGINEERING

INDIAN INSTITUTE OF TECHNOLOGY INDORE

JUNE 2018

Analysis and Design of Wireless Two-Way Relay Networks with Energy Harvesting

A THESIS

Submitted in partial fulfillment of the
requirements for the award of the degree
of
Master of Technology
in
Electrical Engineering
with specialization in
Communication and Signal Processing

by
UGRASEN SINGH

DISCIPLINE OF ELECTRICAL ENGINEERING
INDIAN INSTITUTE OF TECHNOLOGY INDORE
JUNE 2018

INDIAN INSTITUTE OF TECHNOLOGY INDORE

CANDIDATE'S DECLARATION

I hereby certify that the work which is being presented in the thesis entitled **Analysis and Design of Wireless Two-Way Relay Networks with Energy Harvesting** in the partial fulfillment of the requirements for the award of the degree of **MASTER OF TECHNOLOGY** with specialization in **COMMUNICATION AND SIGNAL PROCESSING** and submitted in the **DISCIPLINE OF ELECTRICAL ENGINEERING, Indian Institute of Technology Indore**, is an authentic record of my own work carried out during the time period from May 2017 to June 2018 under the supervision of Dr. Prabhat Kumar Upadhyay, Associate Professor, Discipline of Electrical Engineering.

The matter presented in this thesis has not been submitted by me for the award of any other degree of this or any other institute.

Signature of the student with date
UGRASEN SINGH

This is to certify that the above statement made by the candidate is correct to the best of my/our knowledge.

Signature of the Supervisor of
M.Tech. thesis with date
Dr. PRABHAT KUMAR UPADHYAY

UGRASEN SINGH has successfully given his/her M.Tech. Oral Examination held on **28th June 2018**.

Signature of Supervisor of M.Tech. thesis
Date:

Convener, DPGC
Date:

Signature of PSPC Member
Date:

Signature of PSPC Member
Date:

ACKNOWLEDGEMENTS

My deepest gratitude goes to Dr. Prabhat Kumar Upadhyay for giving me the opportunity to work with him. I have been able to push myself beyond my expectations with his excellent supervision, motivation, encouragement, and personal generosity. He has always been my source of inspiration during my stay at IIT Indore and will be, all my life. I would like to express my sincere appreciation to Dr. Vimal Bhatia and Dr. Surya Prakash for their comprehensive advice and feedback. I also acknowledge Indian Institute of Technology Indore and the Government of India for providing me with financial support.

I would like to thank all the faculties for teaching me during my course work, which laid a strong foundation which eventually has helped me a lot to pursue further research.

My special gratitude for Dr. Devendra S. Gurjar, Mr. Sourabh Solanki, and Mr. Vibhum Singh for providing their help and valuable suggestions both technically and non-technically during my work, they were always there to help me when I needed them.

I am thankful to the entire WiCom research group for directly or indirectly helping me in completion of my project work.

I would also like to thanks my colleagues Piyush, Puneet, Chitresh, Lokesh, Sachin, Bhumi, Kalyani, and Pratistha for making a wonderful company and having fruitful discussions with me.

At last I am indebted to my parents and family members for their unbounded love, endless support and having faith in me, without which this work would not have been possible.

Ugrasen Singh

M.Tech. (Communication and Signal Processing)

mt1602102009

Discipline of Electrical Engineering

IIT Indore

To my beloved ones, for their support and encouragement

Abstract

Modern wireless communication networks are powered by conventional energy sources such as power grids, generators, and rechargeable batteries, as they supply steady energy. However, such energy sources demand regular maintenance or replacement which incurs more operational cost and sometimes may become impractical in hazardous environments. On the other hand, energy harvesting (EH) techniques have been gaining significant attention for complementing the current grid-powered wireless communication networks by prolonging their lifespan and making them more environment friendly. As such, the energy can be harvested opportunistically from the ambient radio-frequency (RF) signals. The basis for such EH lies in a fact that both information and the energy can be transmitted simultaneously through the RF signals. In this thesis, we adopt various EH approaches for the performance analysis of two-way relay (TWR) networks.

Firstly, we analyze the outage performance of TWR networks wherein two communicating nodes exchange their information via a half-duplex battery-enabled relay node. A hybrid decode-amplify-forward based relaying scheme is proposed to make communication links more reliable. In this system setup, the relay node harvests energy from the received RF signals using the time switching based EH approach. Further, it is considered that destination nodes can exploit both direct and relaying links for communication purpose. After the successful EH process, the relay utilizes the harvested energy for processing and broadcasting the received information signals to the destination nodes. At the destination nodes, selection combining (SC) technique has been employed to retrieve the information via direct and relaying links.

Furthermore, we also consider the power splitting approach of EH at the relay node in which the power of received signals is split into the information and the EH seg-

ments. Hereby, relay node harvests energy from the received RF signals in the first two phases and utilizes the harvested energy for information processing and broadcasting in the third phase. Relay node relies on amplify-and-forward operation to broadcast the signals and destination nodes employ the maximum-ratio combining (MRC) technique to combine the signals via direct link as well as relaying link. For this setup, we obtain the expressions for user outage probability, energy efficiency, and achievable system throughput for both MRC and SC schemes under Nakagami-m fading channels. Moreover, we show analytically the importance of considering direct link in the simultaneous wireless information and power transfer in TWR networks.

LIST OF PUBLICATIONS

1. **U. Singh**, S. Solanki, D. S. Gurjar, and P. K. Upadhyay, "Wireless Power Transfer in Two-Way AF Relaying with Maximum Ratio Combining under Nakagami-m Fading", 14th International Wireless Communications and Mobile Computing Conference (IWCMC),Limassol, Cyprus, 25-29 June, 2018.

2. D. S. Gurjar, **U. Singh**, and P. K. Upadhyay, "Energy Harvesting in Hybrid Two-Way Relaying with Direct Link under Nakagami-m Fading", IEEE Wireless Communications and Networking Conference (WCNC), Barcelona, Spain, 15-18 April, 2018.

Contents

List of Figures **vi**

List of Abbreviations **vii**

1 Introduction **1**

1.1 Literature Review 2

1.2 Research Motivation 4

1.3 Contributions 5

1.4 Organisation of the Thesis 6

1.5 Notations 7

2 Background **8**

2.1 Cooperative Communication 8

2.1.1 Relaying Protocols 9

2.2 Diversity Combining Techniques 11

2.2.1 Selection Combining (SC) 11

2.2.2 Maximum Ratio Combining (MRC) 12

2.3 Energy Harvesting (EH) Techniques 13

2.3.1 Time Switching (TS) 15

2.3.2 Power Splitting (PS) 16

2.3.3 Antenna Switching (AS) 16

3 System Model and Description **18**

3.1 Channel Model 18

3.2 System Model 20
3.2.1 Time Switching (TS) Based Relaying Protocol 21
3.2.2 Power Splitting (PS) Based Relaying Protocol 25

4 System Performance Analysis with SC and MRC Schemes 29
4.1 Selection Combining (SC) Scheme 29
4.1.1 Outage Probability (OP) Analysis 29
4.1.2 System Throughput 35
4.2 Maximum-Ratio Combining (MRC) Scheme 35
4.2.1 OP Analysis 35
4.2.2 System Throughput 38
4.2.3 Energy Efficiency 38

5 Numerical and Simulation Results 39
5.1 Hybrid Relaying with SC 39
5.2 AF Relaying with MRC 41

6 Conclusion and Future Works 50
6.1 Conclusion 50
6.2 Future Works 51

REFERENCES 52

List of Figures

2.1 Cooperative network model 9
2.2 Selection combiner 12
2.3 Maximum ratio combiner 13
2.4 A typical RF-EH receiver powering a communication transceiver 14
2.5 A general wireless powered communication network (WPCN). 14
2.6 Time switching architecture. 16
2.7 Power splitter architecture. 16

3.1 Nakagami-m PDF 19
3.2 System model for SWIPT based wireless relaying system. 21
3.3 Frame structure of TS based SWIPT in TWR system. 22
3.4 Signalling in PS-SWIPT based three-phase TWR system. 26

5.1 OP versus SNR curves for $S_b \to S_a$ link with various schemes. 43
5.2 OP versus SNR curves for $S_b \to S_a$ link with different parameters. . . . 44
5.3 Throughput versus SNR curves with different parameters. 45
5.4 Joint effect of r_{th} and α on the system throughput. 46
5.5 OP versus SNR curves of link $S_b \to S_a$. 47
5.6 OP versus ρ curves of link $S_b \to S_a$. 48
5.7 Energy efficiency versus SNR and r_{th}. 49

List of Abbreviations

AWGN	Additive White Gaussian Noise
AF	Amplify-and-Forward
CDF	Cumulative Distribution Function
CSI	Channel State Information
DF	Decode-and-Forward
EH	Energy Harvesting
i.i.d.	Independent and Identically Distributed
IP	Information Processing
IoT	Internet-of-Things
MRC	Maximum-Ratio Combining
MABC	Multiple Access Broadcast
MIMO	Multiple-Input-Multiple-Output
OP	Outage Probability
PSP	Power Splitting Protocol
PDF	Probability Density Function
TSP	Time Switching Protocol
SC	Selection Combining
SNR	Signal-to-Noise Ratio
SISO	Single-Input-Single-Output
TDBC	Time Division Broadcast
TWR	Two-Way Relay
SWIPT	Simultaneous Wireless Information and Power Transfer
WPCN	Wireless Powered Communication Network
WPT	Wireless Power Transfer
WEH	Wireless Energy Harvesting

Chapter 1

Introduction

In the recent past, we have witnessed a remarkable growth of mobile users which is expected to increase even more in forthcoming years owing to the launch of various entertaining and useful social networking sites such as WhatsApp, Instagram, etc. Such remarkable growth in cellular communication has increased the limit of energy consumption in wireless networks. The radio access unit is responsible for 70% to 76% of the total energy consumption due to which the energy production cost increases more than 30% of the total operational cost [1]-[3]. Under these situations, secure and suitable alternative for energy harvesting (EH) is renewable energy (RE) sources such as solar, wind, vibration, thermoelectrical effects, etc. These RE sources for EH depends on their surrounding environment, hence they could be unreliable to provide convenient and perpetual energy supply [4].

Recently, there has been a trend to merge EH schemes into communication networks. As such, simultaneous wireless information and power transfer (SWIPT) [6] and wireless powered communication networks (WPCN) [7] are modern technologies in which EH techniques are integrated to harvest energy from the ambient radio-frequency (RF) signals. Initially, research on wireless EH was concentrated on long-distance and high-power applications, but the severe attenuation of signals and detrimental effects on human health for high power applications at higher frequency averted their further developments. Therefore, the present research on EH is attentive on point-to-point energy transmission through the wireless channel (e.g, used for charging cell-phones,

medical implants, and electrical vehicles). Recently, EH devices are able to harvest microwatt to milliwatt of power over the range of several meters for a transmit power of watts and a carrier frequency less than 30 GHz. Hereby, SWIPT technology has many advantages for wireless communication in terms of spectral efficiency, time delay, energy consumption, and interference management over a wireless channel.

In the era of the Internet-of-Things (IoT), wireless EH scheme can be helpful for powering up the communicating sensor nodes and interchanging data with low power nodes, that support heterogeneous sensor networks. Moreover, the application of SWIPT in future wireless networks with macro cells, massive-MIMO, device-to-device (D2D) and millimeter-wave communication would be helpful to jointly support high throughput and energy substantiality. Consequently, such systems with multiple nodes and antennas consume enormous energy. On the other hand, cooperative relaying has been emerged as a promising strategy to extend the coverage and overcome the losses due to the various factors, including fading and interference. The most known relaying strategies are amplify-and-forward (AF), decode-and-forward (DF), and compressed-and-forward (CF). Further, achievable throughput of SWIPT in relaying protocols as time switching (TS) relaying and power switching (PS) relaying in the delay-limited and delay-tolerant destinations have been investigated. EH in multiple relay system with an analog network coding based on two-way relay (TWR) system has been studied in[7].

1.1 Literature Review

The wireless EH receiver design is an important task in the wireless networks, in which the information and EH receivers are expected to utilize the same single antenna or multiple antennas. To fulfil the quality of service (QoS) measure BER, Capacity, etc., different tradeoffs are analyzed in the physical layer concerning the EH techniques. In this thesis, TS and PS techniques have been adopted for EH. Recently, research on the EH techniques for point-to-point communication for single and multiple antenna systems in the wireless faded channels have been proposed in [2], [5]. The EH has been

emerged as one of the promising technologies driving cooperative relay networks, sensor networks, and IoT networks. To enable sustainable and ubiquitous communications, SWIPT scheme has been introduced, where nodes are capable to harvest energy from the RF signals [8]. This scheme utilizes the idea that both energy and information signals can be transmitted through RF signals at the same time. Two practical receiver designs based on TS and PS techniques were proposed to realize SWIPT in the wireless system [10],[11]. A unique work for the dynamic power splitting was proposed in [10], i.e., based on on-off power splitting technique.

On another front, cooperative relying systems have been explored in many literatures, due to its ability of providing wide coverage, capacity, and improved link reliability [9], [12]. Among them, TWR is the most popular and spectral-efficient scheme. In this scheme, two end-to-end parallel communications can be realized in just two-time phases [14], [15]. The main issue with TWR scheme is its inability to exploit direct link due to half-duplex nature of the nodes [16]. To utilize the benefits of both TWR and direct link, researchers (see [17] and the references therein) investigated another relaying technique named as time-division broadcast (TDBC) protocol. Unlike TWR, in TDBC protocol, the system requires an additional phase to accomplish two end-to-end information exchange with improved link reliability. Owing to the potential features of SWIPT, several research works adopted it in the relay-based wireless systems. For instance, authors in [19]-[26] combined the EH and signal processing mechanism in the single antenna system and then presented a time switching-based network coding relaying (TSNCR) protocol for the TWR system. Moreover, authors introduced the concept of SWIPT with AF based TWR system to improve the spectral efficiency. More specifically, authors in [21] adopted TS based EH approach at the relay node and analyzed the outage performance, whereas, authors in [24] focused on optimizing the problem of power splitting and relay processing matrix for TWR systems. Recently, to exploit the benefits of the direct link, few works [25], [26] have considered EH in the three-phase TWR system. In [25], authors have proposed different wireless power transfer (WPT) policies for TS based two-phase and three-phase (IP phases) AF-TWR system. Further, the expressions of the outage probability (OP) and overall throughput for three-phase

DF-TWR system with EH have been derived in [26]. More importantly, authors in [26] have not considered the direct link for investigating the system performance. Both these works have adopted either AF or DF relaying scheme for analyzing the system performance. Different from AF-based TWR system, research works in [27] and [28] considered DF-based relaying approach for SWIPT-enabled TWR system. In particular, authors in [27] investigated SWIPT-based two-way DF relay network and analyzed their performance in terms of achievable sum-rate. Further, the outage performance of this system with asymmetric traffic patterns was analyzed in [28] by considering both TS and PS techniques for EH. The wireless EH network with time-varying co-channel interferences in the fading channel was studied in [29].

In [30], author proposed the training assisted PS receiver to enhance the system performance. Here, the receiver uses a different power splitting ratio for the training phase and information phase to achieve the better data rate. Moreover, a non-adaptive and adaptive power splitting approaches are used. For the non-adaptive power splitting, the power splitting ratio is fixed, whereas for adaptive power splitting, the power splitting ratio is changeable. Thereby, it has been proved that the adaptive power splitting approach outperforms the non-adaptive power splitting approach.

1.2 Research Motivation

The main inspiration behind this research in wireless EH is to prolong the lifetime of the WCN by replacing the traditional energy sources with the EH sources. When WCN is powered by traditional energy sources such as power-grid and batteries, networks face critical problem of unexpected disruption of operation due to the power cut and/or discharging of batteries. Moreover, these energy sources require continuous maintenance which incurs high cost. In addition, the conventional wireless networks also consume more power. Owing to these reasons, we need to develop a network that can reduce the energy consumption, and which can also be powered by low energy sources. These are main motivations that cause the flurry of research activity in a new scheme called EH that is emerging as a highly attractive form of green communication. Harvesting energy

from RE sources is random over the time owing to its stochastic nature. Moreover, EH from RE totally depends on its surrounding environment. If atmospheric conditions are not good enough, then these methods will not be able to harvest energy efficiently. Therefore, traditional EH scheme is not applicable everywhere, which finally motivates this work towards the concept of EH from the RF signals. In RF-based EH techniques, the RF energy is ultimately converted into electrical energy. Thus, harvesting energy from RF signals promises a wide scope for the replacement of small batteries in low power electrical devices and systems.

In recent years, the global mobile subscribers are growing rapidly which further increases energy consumption of mobile networks and demands for higher data rate. To accomplish their demands, it requires more energy which have been realized from traditional energy sources such as fossil-fuel and coal. Aforementioned traditional energy sources are hazardous and costly, owing to this reason, we need to focus towards EH techniques. Wireless EH techniques are environment-friendly and cheap. Hereby, this new concept of EH can be used in cooperative communication networks, in which relay transmission can be powered by RF-based EH signals. EH system portrays a signal that releases electrical energy from one place which is further captured on the another place without the use of any wire or any other supporting medium.

1.3 Contributions

The major contributions of the thesis are described as follows:

- The leading concept of the thesis is the design of a bidirectional cooperative network with wireless EH receiver at the relay node. The considered network comprises two source-destination nodes pair communicating with each other via an EH rechargeable relay node, where relay node utilizes the harvested energy for information transmission.

- Further, TS and PS based relaying protocols are adopted for EH and IP at the relay node in addition with hybrid amplify-decode-forward relay operation. Moreover, in order to enhance the transmission reliability in TWR networks, direct link

is exploited for transmission between source and destination nodes by using the TDBC transmission protocol.

- Furthermore, for TS protocol, analytical expressions for the user OP and the system throughput are derived using hybrid relaying under the Nakagami-m fading channels. Hereby, at the destination nodes, SC scheme is employed to make the use of intended signals received via relay and direct links.

- Later, closed form expression for the user OP is derived at the destination nodes using AF relaying technique under Nakagami-m fading channels. At the destination nodes, MRC technique is employed to make use of intended signals received via relay and direct links. Moreover, expressions for system throughput and energy efficiency are derived assuming a delay limited transmission mode. Thereby, it can be inferred that point-to-point cooperative communication PS technique always achieves higher energy-rate pairs than the TS technique. Moreover, after comparison, it can be shown that MRC technique outperforms the SC technique.

1.4 Organisation of the Thesis

The rest of this thesis is organized as follows: In Chapter 2, the cooperative communication and EH schemes for the considered system model are discussed. Further, Chapter 3 provides information about the system model, which is useful for analysis of the system in subsequent chapters. The stochastic modeling of the wireless channel under Nakagami-m fading is also done in this chapter. Furthermore, Chapter 4 shows the performance analysis of the considered system by deriving expressions for OP, throughput, and energy efficiency considering both SC and MRC receivers at the destination nodes. Chapter 5 presents the simulation and analytical results of the proposed model. Finally, Chapter 6, includes conclusion and scope of the future work of this thesis.

1.5 Notations

Throughout this thesis, $f_X(\cdot)$ and $F_X(\cdot)$ signify the probability density function (PDF) and the cumulative distribution function (CDF) of a random variable X, respectively, and $\Pr[\cdot]$ denotes probability. $\Gamma[\cdot,\cdot]$, $\Upsilon[\cdot,\cdot]$, and $\Gamma[\cdot]$ represent, respectively, the upper incomplete, the lower incomplete, and the complete gamma functions [34, eq. (8.350)]. $\mathcal{K}_v(\cdot)$ denotes vth order modified Bessel function of second kind [34, eq. (8.432.1)], $\Psi[\cdot]$ represents digamma function [34, eq. (8.365.4)], whereas $\mathcal{W}_{u,v}(\cdot)$ represents Whittaker function [34, eq. (9.222)].

Chapter 2

Background

In this chapter, we resume the development of background materials necessary for a more detailed understanding of the cooperative communication systems. In addition, we will study various EH techniques used in the wireless communication systems.

2.1 Cooperative Communication

In wireless communication, growing demands for data rate have pushed us towards the use of advanced algorithms and techniques which increases the data rate while ensuring the QoS required for different applications. To improve the performance of system, various important techniques such as modulation, coding, multiplexing, OFDM, MIMO, and spatial diversity have been used in current wireless networks. Amongst these, MIMO is one of the most effective techniques for improving the link reliability and for fulfilling the user demands by offering excellent diversity gain over the SISO system without increasing power and bandwidth. Although, the MIMO scheme has numerous advantages at base station, it has deployment issues in small-sized devices. As wireless communication system suffers from fading effect, MIMO efficiently combats the effect of fading by providing multi-path diversity. Some common diversity schemes are time diversity, frequency diversity, transmitter diversity, and spatial diversity. Specifically, spatial diversity is realized by transmitting signals from different places to obtain the independently faded form of signals at the receiver by using multiple antennas. However,

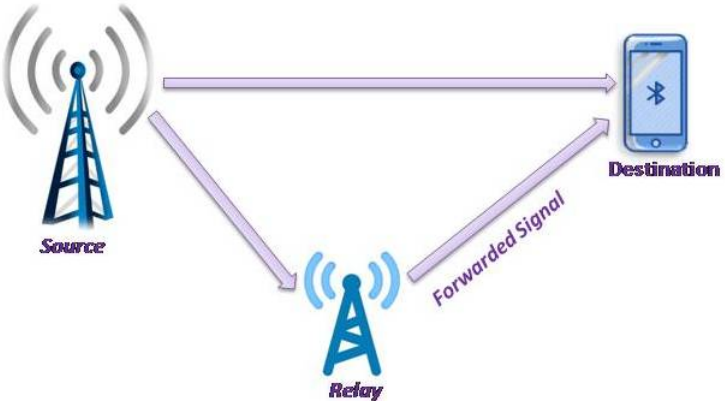

Figure 2.1: Cooperative network model

achieving spatial diversity using MIMO technique is not efficient and even infeasible, in some situations, due to setup of multiple antennas. To overcome this, another form of spatial diversity known as cooperative diversity [31] had been proposed, in which diversity gains are achieved via cooperation among the users. The schematic diagram of a basic cooperative network is shown in Fig. 2.1

Cooperative networks allow the single antenna users to share their antennas in a multi-user environment and create a virtual multiple-antenna transmitter that allows them to achieve transmission diversity. As depicted in Fig. 2.1, a source base station communicates with a destination node using an intermediate relay node which facilitates the cooperative transmission of signal to the destination together with a direct link transmission. This technique helps in improving the link connectivity, spectral efficiency, and improving the communication link reliability of the wireless networks. As such, cooperative diversity technique is favourable due to its easy deployment and cost effective implementation.

2.1.1 Relaying Protocols

When a signal is received at the relay node from the source, the relay processes the received signal before sending it to the destination. Based on the processing at the relay node, relaying protocols can be broadly categorized into two types viz., fixed relaying and adaptive relaying. In what follows, we explain both of these techniques for single relay cooperative networks.

1. Fixed Relaying

In this relaying protocol, wireless channel characteristics between source and relay are deterministic. Fixed relaying becomes more important when channel between source and relay is in deep fading. In such scenario, relay effectively processes the information and retransmits to the destination. There are two most commonly used techniques under fixed relaying which are described below in detail.

a) Amplify-and-Forward (AF)

In AF relaying scheme, the relay scales the received signal, amplify it, and then forwards the amplified version of the scaled signal to the destination. More specifically, the amplification is performed at the relay node to remove the effects of channel fading from the signal of the source to relay link. However, in this technique, the relay node amplifies the received signal as well as the noise, which is the main drawback of this scheme. Whereas, the main advantage is reduced hardware designing complexity over the other relaying protocols.

b) Decode-and-Forward (DF)

This relaying protocol is also known as the pulse reshaping relaying. In DF relaying protocol, relay fully decodes the received information signal from the source and forwards the re-encoded version of the signal to the destination. However, in this case, there are more chances of error in decoding at the relay node. Error correcting code is one of the possible ways to reduce the possibility of decoding error at the relay node.

To overcome the drawbacks of aforementioned relaying techniques, adaptive relaying technique had been introduced as explained below.

2. Adaptive Relaying

In this case, the channel information is available at the relay node such that it can adjust its performance according to the channel states of the source-relay link. It can be further categorized into two types as following.

a) Selective Relaying

In this scheme, since the channel coefficient is known at the receiver, the relay can change its transmission properties according to the perceived channel states. Whenever,

the measured SNR at the relay exceeds the certain level, relay node performs the fixed relaying techniques to process the received information. And when the measured SNR lies below the certain level, the source can be asked for the repetition of more powerful codes to continue the transmission to the destination.

b) Incremental Relaying

This scheme uses the feedback link from the destination node. The relay can either forward the received signal from the source or stay idle. If the destination acknowledges the failure of the direct link, then only relay node can forward the received information. Therefore, this incremental relaying will improve spectral efficiency over fixed and selective relaying.

2.2 Diversity Combining Techniques

In wireless communication, signals are propagated from the source to the destination via multipath propagations. Due to the multipath propagation of signals, they experience fading at the receiver over the time and space. To overcome this effects of fading, diversity techniques are used. A diversity technique is based on the mechanism where the receiver gets several copies of the signal to convey the same information through the channels which are independently faded. It can be achieved in three different domains: time, frequency, and space. In order to achieve the diversity gain, multiple copies of the independent received signal have to be combined, and such combining improves the performance of the diversity technique. There are several kinds of diversity combining techniques exist such as SC, MRC, equal gain combining (EGC), and hybrid combining (two different forms). In our work, we have considered the SC and MRC techniques.

2.2.1 Selection Combining (SC)

In SC technique, out of all the available signals at the receiver, we select the signal having maximum instantaneous SNR at the output using switching circuit. There is no need to connect each channel output, as it gives the lower bound of diversity combining.

System model for the SC is given in Fig. 2.2.

$$\mathbf{y} = \mathbf{h}x + \mathbf{n}, \tag{2.1}$$

$$\gamma = \max_{i \in \{1,2,....L\}} [\gamma_i], \tag{2.2}$$

$$\gamma_i = \frac{P|h_i|^2}{\sigma^2}, \tag{2.3}$$

where $\mathbf{y}=[y_1, y_2.....y_L]^t$ is the received signal vector, $\mathbf{h}=[h_1, h_2.....h_L]^t$ is the channel coefficient vector, $\mathbf{n}=[n_1, n_2.....n_L]^t$ is the AWGN vector, γ_i is the instantaneous SNR of the i^{th} branch, P is the signal power, and σ^2 is the noise power.

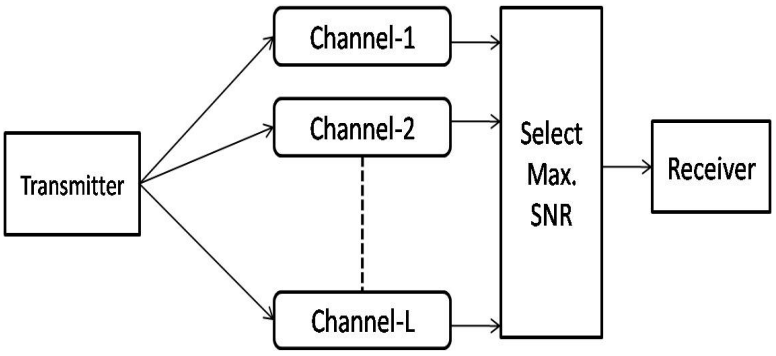

Figure 2.2: Selection combiner

2.2.2 Maximum Ratio Combining (MRC)

In SC, branch with the highest instantaneous SNR is selected. However, this is not an optimal solution due to the ignorance of remaining branch SNRs. In MRC, multiple copies of the signal which are conveying the same information are multiplied by weight vector and combined to maximize the instantaneous SNR at the output. Therefore, this scheme is more helpful to eliminate the effect of fading and interference over the received signal and optimizes the performance of antenna array system. Hence, the performance of MRC is considered as the upper bound among all the possible combining techniques. The architecture of MRC combiner circuit is shown in Fig. 2.3 which illustrates that output signal is the weighted sum of the signal from L links. The received signal at the

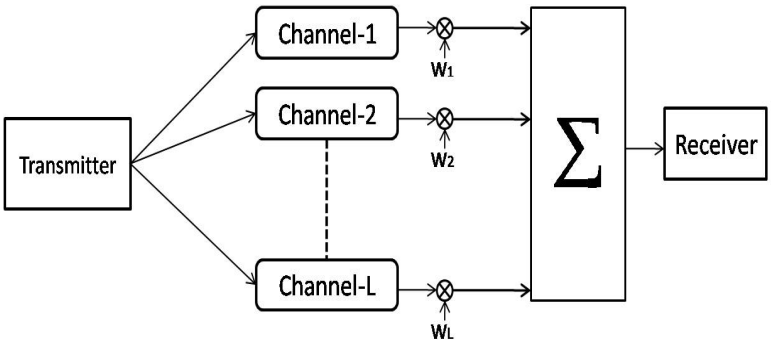

Figure 2.3: Maximum ratio combiner

receiver is represented as vector $\mathbf{y}$, and output signal is as vector $\mathbf{r}$, and are given as

$$\mathbf{y} = \mathbf{h}x + \mathbf{n}, \tag{2.4}$$

$$\mathbf{r} = \mathbf{w}^H\mathbf{y} = \mathbf{w}^H\mathbf{h}x + \mathbf{w}^H\mathbf{n}. \tag{2.5}$$

Where $\mathbf{y}$=$[y_1, y_2.....y_L]^t$ is the received signal vector, $\mathbf{h}$=$[h_1, h_2.....h_L]^t$ is the channel coefficient vector, $\mathbf{n}$=$[n_1, n_2.....n_L]^t$ is the AWGN vector, and $\mathbf{w}$=$[w_1, w_2.....w_L]^t$ is the weight vector.

The instantaneous output SNR is,

$$\gamma = \frac{P|\mathbf{w}^H\mathbf{h}|^2}{\sigma^2\mathbf{I}_L}. \tag{2.6}$$

To maximize the SNR at the receiver, $\mathbf{w}$ should be equal to the $\frac{\mathbf{h}}{||\mathbf{h}||}$ so that

$$\gamma = \frac{P|\frac{\mathbf{h}^H}{||\mathbf{h}||}\mathbf{h}|^2}{\sigma^2\mathbf{I}_L} = \sum_{i=1}^{L}\frac{P|h_i|^2}{\sigma^2}. \tag{2.7}$$

Hereby, the output SNR is the sum of the SNRs by individual received signal components.

2.3 Energy Harvesting (EH) Techniques

RF-based EH is the act of scavenging energy from the ambient RF signals and the dedicated RF signals by the EH devices. RF energy signals are transmitted over the

wireless channel which further experience fading at the receiver end due to multipath propagation in the wireless channel. Owing to this reason, wireless EH technique is more efficient for lower distance communication for powering up the wireless nodes which are spread over an open area. There are many application of wireless EH such as charging of the mobile phones, medical equipments, electrical vehicles, and wireless sensor networks. In Fig. 2.4, a typical RF-based EH receiver is shown which consists of a receiver antenna, a matching circuit, RF-to-direct current (DC) converter/rectifier, and energy storage unit [32]. The matching circuit is able to operate in diverse frequency bands to harvest energy from various RF sources and maximizes the power transfer from the antenna to the rectifier circuit (RF-to-DC converter). The output DC voltage of the rectifier circuit is either used for recharging the battery or powering up the information processing unit directly.

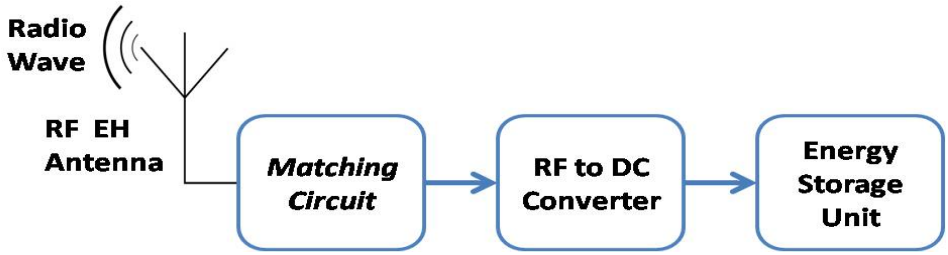

Figure 2.4: A typical RF-EH receiver powering a communication transceiver

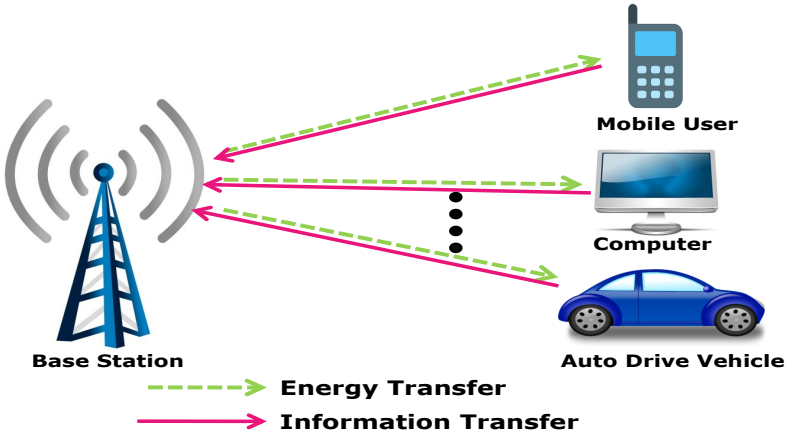

Figure 2.5: A general wireless powered communication network (WPCN).

In RF-based EH, the total harvested energy, represented by E_h, can be obtained from the Friis equation [**?**], which depends on the transmitted power, carrier wavelength,

and the distance between the transceivers. It can be given as

$$E_h = cos^2(\phi)\frac{P_t G_t G_r \lambda^2 \eta \tau}{(4\pi d)^2}, \tag{2.8}$$

where P_t represents the transmit power, G_t represents the transmitter antenna gain, G_r represents the receiver antenna gain, λ is the signal wavelength, d is the distance between transmitter and receiver, η is the efficiency of RF-to-DC converter circuit, τ is time duration of energy transfer, and $\cos(\phi)$ is the polarization loss factor. We can observe from the eq. (2.8) that G_r, G_t, and directive gain have to be increased in order to increase the harvested energy E_h. To obtain high directive gain, an omni-directional antenna can be used at the receiver end to maximize the harvested energy. Another most critical part of the EH system is RF-to-DC conversion system and its designing is more complex. The RF-to-DC conversion efficiency of the system directly affects the received energy.

Fig. 2.5 illustrates the wireless powered networks where terminal users in the networks harvest energy from the base station to establish the communication between transceivers. In the first mode, terminal users harvest the RF energy from the base station (BS) and then utilize this harvested energy to forward the information. In the second mode, the information and power is transmitted simultaneously toward users, which is split at the receiver end to harvest energy and process information at separate antennas. This technique is known as SWIPT. There are various EH techniques to harvest energy in different domains (time, power, antenna, space) exist. But, we have considered only time and power domain technique to harvest energy in our thesis.

2.3.1 Time Switching (TS)

The TS technique schedules distinct time slots for arriving signal to harvest energy and process information simultaneously [11], [30] in the period of one transmission block. In this scheme, the signal splitting is executed in the time domain and thus the whole signal energy received in time slot is either used for EH or IP. A schematic diagram of this scheme is shown in Fig. 2.6. The hardware implementation of this technique at

the receiver is more efficient and reliable, but it requires accurate time synchronization between the EH and IP receivers. All the harvested energy in EH phase is stored in the energy storage unit for the future use.

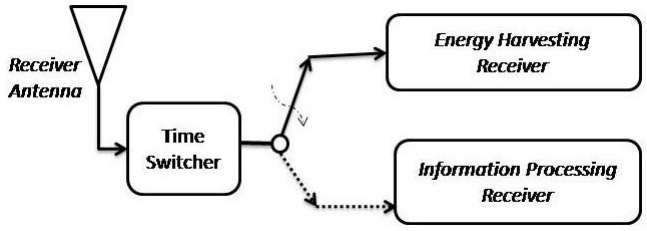

Figure 2.6: Time switching architecture.

2.3.2 Power Splitting (PS)

The PS scheme divides the signal into two streams of different power levels using the power splitter mechanism, one component of the signal is used for EH and another is used for IP [11]. The hardware implementation of the proposed scheme is more complex as compared to TS scheme as it needs to optimize the power splitting factor α. Therefore, it is more suitable for lower data rate in delay limited transmission, due to simultaneous transmission of information and power. The schematic diagram of the PS scheme is shown in Fig. 2.7 .

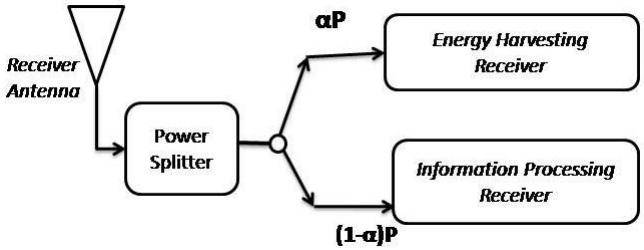

Figure 2.7: Power splitter architecture.

2.3.3 Antenna Switching (AS)

In this scheme, an array of antenna system is used to harvest energy from the RF signal for reliable device operation. In a system utilizing SWIPT technique, each antenna

element dynamically switches between EH/IP in its antenna domain. The receiver antenna is divided into two types, where one type is used for IP and the other type for EH. The AS technique is used in MIMO relay channel where relay node utilizes the harvested power for forward mode operation.

Chapter 3

System Model and Description

In this chapter, we describe the TWR system model with EH. The model proposed here will be used for all the investigation in subsequent chapters. First, we discuss in detail the wireless channel model and its various property matrices viz., PDF, CDF, etc. Further, system model and its peripheral components are described.

3.1 Channel Model

In wireless communication, channel plays an important role in establishing successful communication between transmitter and receiver. The characteristics of wireless channel depend upon the distance between transceivers, path of the wave propagation, and the obstacles around the path. This channel model is focused on predicting the average signal strength at the receiver. Due to multipath propagation, the rapid fluctuations of the channel is described in our model by Nakagami-m distribution. It is a more generalized distribution, which offers good approximation for widely varying wave propagation path scenarios by varying single parameter *"m"*. Nakagami-m [33] has described that the signal amplitude fading in radio wave propagation can be well modeled by its PDF, as shown in Fig. 3.1.

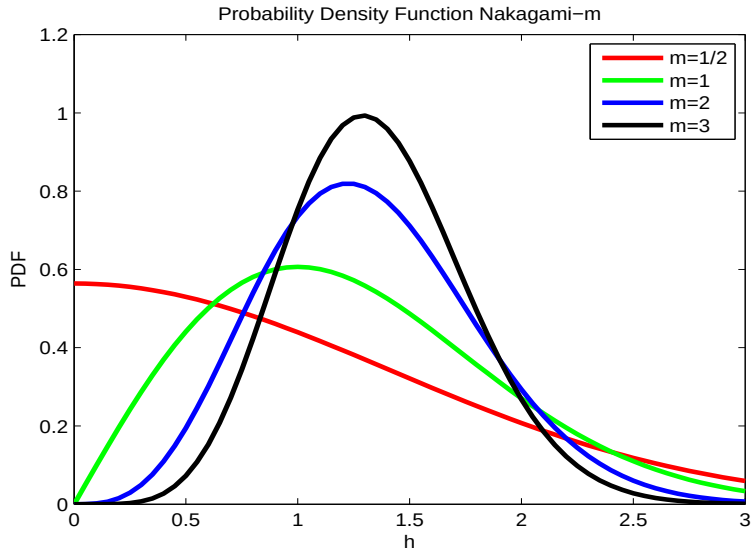

Figure 3.1: Nakagami-m PDF

$$f_{\tilde{h}}(h,m,\Omega) = \begin{cases} \frac{2}{\Gamma(m)}\left(\frac{m}{\Omega}\right)^m h^{2m-1} e^{-\left(\frac{mh^2}{\Omega}\right)} & \text{for } h \neq 0, \\ 0 \qquad \text{for } h = 0, \end{cases} \tag{3.1}$$

where $\Omega = \mathrm{E}[\tilde{h}^2]$ with $\mathrm{E}[\cdot]$ as the expectation operator, $m = \frac{\Omega^2}{Var[\tilde{h}^2]} \geq \frac{1}{2}$, $\tilde{h}$=$\sqrt{h_1^2 + h_2^2 + h_3^2 + ...h_n^2}$. Here, h_i, $i = 1, 2, ...n$, are independent and identical distributed (i.i.d) RVs with zero mean and variance σ_h^2. Different values of m can realize different fading scenarios as follows

m=1: Rayleigh fading

$m \to \infty$: Gausian PDF

m=$\frac{1}{2}$: One-sided Gaussian fading, the worst fading condition.

Another way of representing the statistical characteristics of RVs is known as CDF, and is obtained by integrating the PDF over the defined limit. It can be given as

$$F_{\tilde{h}}(h,m,\Omega) = \begin{cases} \frac{1}{\Gamma(m)} \Upsilon\left(m, \frac{mh}{\Omega}\right) & \text{for } h \neq 0, \\ 0 \qquad \text{for } h = 0, \end{cases} \tag{3.2}$$

where $\Upsilon(.)$ is represents the lower gamma function.

If a random variable X is defined as $X = |\tilde{h}|^2$. Its PDF follows the gamma distribution

function, which can be expressed as

$$f_X(x, m, \Omega) = \begin{cases} \frac{1}{\Gamma(m)} \left(\frac{m}{\Omega}\right)^m x^{m-1} e^{-\left(\frac{mx}{\Omega}\right)} & \text{for } x \neq 0, \\ 0 \qquad \text{for } x = 0, \end{cases} \tag{3.3}$$

which is used for further analysis of system performance in next subsequent chapters.

3.2 System Model

The system model shown in Fig. 3.2, allows a point-to-point communication between two users. The distance between S_a and S_b is such that direct transmission is possible between them. We consider a SWIPT-enabled TWR system, where two source nodes S_a and S_b communicate with each other with the aid of a battery-enabled relay node R. All participating nodes are assumed to operate in half-duplex mode and equipped with single antenna devices. We propose two EH stratgies to harvest energy from RF signals viz., TS and PS, at the relay node. In TS strategy, one block duration is divided into two phases, i.e., EH phase and information processing (IP) phase. During EH phase, relay node harvests energy from the transmitted signals from the two source nodes and stores this energy for broadcasting the signals. The bidirectional information exchange between two source nodes is performed in three IP phases using HDAF relaying. In first IP phase, S_a transmits its signal to another source node S_b and relay node. Likewise, in second IP phase, S_b transmits its signal to S_a and R. Thereafter, R first tries to decode both the received signals intended for S_a and S_b, respectively, and then it will apply XOR based encoding to perform DF operation and broadcast the combined signal using harvested energy. If R fails to decode any signal, then it will apply AF operation to broadcast the combined signal.

Based on PS strategy, one block duration is divided in three IP phases, where power splitter splits the received signal power by a factor ρ for the EH and by $(1-\rho)$ for IP. For the first two subsequent phases, relay node R harvests the energy ρP_r^I and ρP_r^{II} from the source nodes S_a and S_b respectively. In the third IP phase, relay node utilizes all the harvested energy to broadcast the combined signals after applying the AF operation.

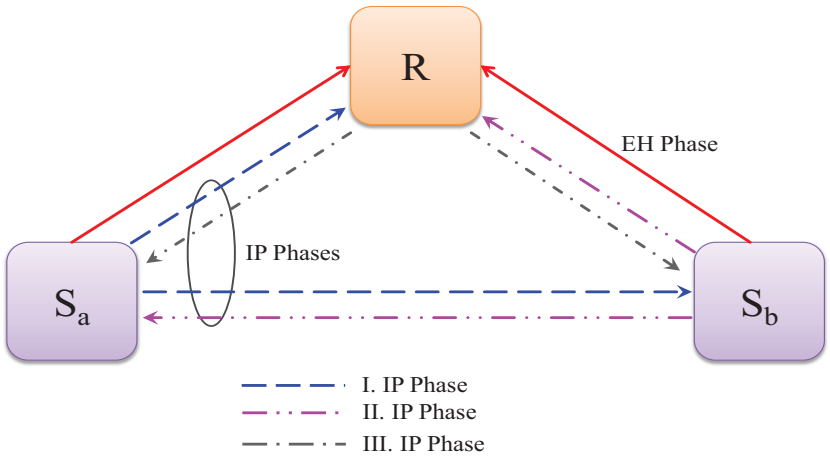

Figure 3.2: System model for SWIPT based wireless relaying system.

We assume that all the channel coefficients undergo quasi-static fading, where channel condition remains unchanged for one block duration T. We denote channel coefficients between source node S_i to relay node R and R to S_i as $h_{i,r}$ and $h_{r,i}$, respectively, for $i \in \{a, b\}$. The channel coefficients of both hops $h_{i,r}$ and direct link $h_{i,j}$ follow the reciprocity and undergo Nakagami-m distribution with average power Ω_i and Ω_d and severity parameters m_i and m_d, respectively. The channel coefficients are assumed to be quasi-static block-fading channels and channel state is constant over a transmission block time T. The comprehensive analysis of the proposed TS and PS relaying protocols is described in the subsequent sections.

3.2.1 Time Switching (TS) Based Relaying Protocol

Considering TS, as discussed in Section 2.3.1, the signal transmission process for EH and IP at the relay node is discussed in this section. As shown in Fig.3.3 , one transmission block duration T is divided into two phases i.e., αT and $(1-\alpha)T$, where $0 < \alpha < 1$. In the first phase or EH phase, αT is dedicated for harvesting energy from RF signals transmitted by the two source nodes. In the second phase, $(1-\alpha)T$ is used for information processing and signaling. It is further divided into three equal phases (IP phases). The choice of α reflects the amount of harvested energy at the relay node, therefore it can be crucial to maintain the tradeoff between link reliability and

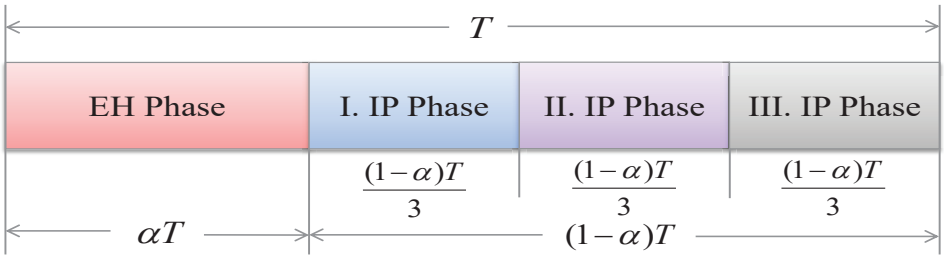

Figure 3.3: Frame structure of TS based SWIPT in TWR system.

achievable throughput of the system.

Energy Harvesting (EH)

In the EH phase, relay receiver rectifies the received RF signal into direct current to charge up the battery. The received signal y_r at the relay node can be expressed as

$$y_r = \sqrt{P_a} h_{a,r} x_a + \sqrt{P_b} h_{b,r} x_b + n_r, \tag{3.4}$$

where x_i, for $i \in \{a, b\}$, are the normalized information symbols from the node S_a and node S_b, respectively; n_r represents the AWGN with zero mean and variance σ_r^2.
In EH phase, the harvested energy can be expressed as

$$E_h = \eta \alpha T (P_a |h_{a,r}|^2 + P_b |h_{b,r}|^2), \tag{3.5}$$

where $0 < \eta < 1$ denotes the energy conversion efficiency of EH circuit, and $P_a \,\&\, P_b$ are transmit powers at $S_a \,\&\, S_b$, respectively. By utilizing (3.5), transmit power at the relay node can be expressed as

$$P_r = \frac{3\eta\alpha}{1-\alpha} (P_a |h_{a,r}|^2 + P_b |h_{b,r}|^2). \tag{3.6}$$

Here, we have assumed that the power used for signal processing is negligible as compared to the power used for signal transmissions, as adopted in [11].

Information Processing (IP)

After EH phase, let S_a transmits unit energy symbol x_a in the first IP phase, then the received signals at S_b and R can be expressed, respectively, as

$$y_{a,b} = \sqrt{P_a} h_{a,b} x_a + n_b \tag{3.7}$$

and

$$y_{a,r} = \sqrt{P_a} h_{a,r} x_a + n_r, \tag{3.8}$$

where $n_b \sim \mathcal{CN}(0, \sigma_b^2)$ and $n_r \sim \mathcal{CN}(0, \sigma_r^2)$ are additive white Gaussian noise (AWGN) variables at S_b and R, respectively.
Likewise, in second IP phase, S_b transmits unit energy symbol x_b. The received signals at the other nodes can be given as

$$y_{b,a} = \sqrt{P_b} h_{b,a} x_b + n_a \tag{3.9}$$

and

$$y_{b,r} = \sqrt{P_b} h_{b,r} x_b + n_r, \tag{3.10}$$

where $n_a \sim \mathcal{CN}(0, \sigma_a^2)$ is AWGN at S_a. After receiving the signals in first and second IP phases, the relay node first tries to decode both x_a and x_b, and after that, it will broadcast these signals (x_a and x_b) by applying one of the following two relaying operations adaptively in the third IP phase.

1) *Decode-and-Forward (DF):* In Section 2.1.1, we have studied the details of DF relaying protocol. Herein, relay node performs the DF-based operation when it successfully decodes both signals (x_a and x_b) received in first and second IP phases. If both signals are decoded successfully, the relay node applies bit-wise XOR operation to obtain re-encoded symbol ($x_a \oplus x_b$) which will be used for signal broadcasting in

third IP phase. Thereby, the received signal at source nodes S_i, for $i \in \{a, b\}$, can be expressed as

$$y_{r,i}^{\mathrm{DF}} = \sqrt{P_r} h_{r,i}(x_a \oplus x_b) + n_i, \tag{3.11}$$

where $n_i \sim \mathcal{CN}(0, \sigma_i^2)$ is AWGN at S_i and P_r is transmit power at relay node.

2)*Amplify-and-Forward (AF):* We have discussed about AF relaying protocol in Section 2.1.1. Hereby, when the relay node fails to decode any of the two signals (x_a or x_b), it combines the two signals received in first and second IP phases and then applies AF operation to broadcast the combined signal. Using (3.8) and (3.10), the transmitted signal from the relay node can be expressed as

$$x_{r,i}^{\mathrm{AF}} = \mathcal{G}(y_{a,r} + y_{b,r}), \tag{3.12}$$

where $\mathcal{G} = \sqrt{P_r/(P_a|h_{a,r}|^2 + P_b|h_{b,r}|^2 + 2\sigma_r^2)}$ is a gain of the relay node.
Now, the received signal at source node S_i can be given as

$$y_{r,i}^{\mathrm{AF}} = h_{r,i}\mathcal{G}(\sqrt{P_a} h_{a,r} x_a + \sqrt{P_b} h_{b,r} x_b + 2n_r) + n_i. \tag{3.13}$$

SNR Analysis

We first compute the instantaneous SNRs of the $S_a \longrightarrow S_b$ and $S_a \longrightarrow R$ links. Based on (3.7) and (3.8), the SNRs at S_b and R, in first IP phase, can be given, respectively, as

$$\begin{aligned} \gamma_{a,b} &= \frac{P_a|h_{a,b}|^2}{\sigma_b^2}, \\ \text{and} \qquad \gamma_{a,r} &= \frac{P_a|h_{a,r}|^2}{\sigma_r^2}. \end{aligned} \tag{3.14}$$

Next, we compute the instantaneous SNRs of the $S_b \longrightarrow S_a$ and $S_b \longrightarrow R$ links. On utilizing (3.9) and (3.10), the corresponding SNRs at S_a and R, in second IP phase,

can be given, respectively, as

$$\gamma_{b,a} = \frac{P_b|h_{b,a}|^2}{\sigma_a^2},$$
$$\text{and} \qquad \gamma_{b,r} = \frac{P_b|h_{b,r}|^2}{\sigma_r^2}. \tag{3.15}$$

In the third IP phase, relay node broadcasts the received information. As both source nodes know their own transmitted signals, therefore, they can cancel the self-interference from (3.11). After canceling the self-interference, the SNR expression at S_i can be given as

$$\gamma_{r,i}^{\text{DF}} = \frac{(\varepsilon_i|h_{i,r}|^2 + \varepsilon_\jmath|h_{\jmath,r}|^2)|h_{r,i}|^2}{\varphi}, \tag{3.16}$$

where $\varphi = (1-\alpha)/3\eta\alpha$, $\varepsilon_i = P_i/\sigma_i^2$, and $\varepsilon_\jmath = P_\jmath/\sigma_i^2$, for $i, \jmath \in \{a, b\}$ with $i \neq \jmath$.

After canceling the self-interference term from (3.13) and applying the approximation $(P_a|h_{a,r}|^2 + P_b|h_{b,r}|^2 + 2\sigma_r^2) \approx (P_a|h_{a,r}|^2 + P_b|h_{b,r}|^2)$, the SNR expression at source node S_i can be given as

$$\gamma_{r,i}^{\text{AF}} = \frac{\xi_i|h_{r,i}|^2|h_{\jmath,r}|^2}{2|h_{r,i}|^2 + \omega_i}, \tag{3.17}$$

where $\xi_i = P_\jmath/\sigma_r^2$ and $\omega_i = (1-\alpha)\sigma_i^2/3\eta\alpha\sigma_r^2$, for $i, \jmath \in \{a, b\}$, with $i \neq \jmath$. In fact, the approximation utilized to derive (3.17) leads to accurate results over entire SNR region.

3.2.2 Power Splitting (PS) Based Relaying Protocol

In Section 2.3.2, we have discussed in detail about the PS-based relaying operation. Here, we are using PS based relay in a cooperative communication system wherein a transmission block is divided into three-phases. We have shown in Fig. 3.4, the communication block diagram denoting the PS relaying protocol where relay splits the received signal in first two information processing phases. During the first two consequent phases of the block time, the fraction of power ρP_i is used for energy harvesting and remaining power $(1-\rho)P_i$ is used for information processing, where $0 \leq \rho \leq 1$, $i \in \{a, b\}$. It

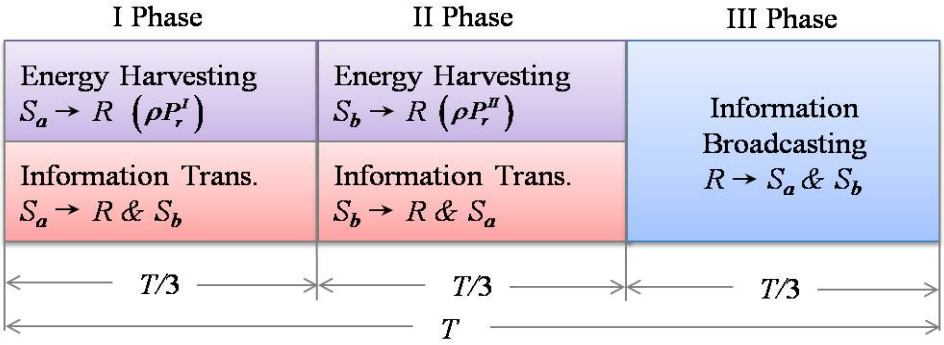

Figure 3.4: Signalling in PS-SWIPT based three-phase TWR system.

is assumed that all the harvested energy is utilized by the relay for broadcasting the information signal to the destination. We now analyze the EH and IP at the relay node for PS relaying protocol.

EH and IP

In the considered SWIPT-based relay system, a power splitter is used to split the received signal in the ratio $\rho : (1-\rho)$. Let S_a transmits unit energy symbol x_a in the first phase. The received signal at relay node R and source node S_b can be expressed, respectively, as

$$y_{a,r}^I = \sqrt{P_a} h_{a,r} x_a + n_r^I \tag{3.18}$$

and

$$y_{a,b}^I = \sqrt{P_a} h_{a,b} x_a + n_b^I, \tag{3.19}$$

where P_a represents transmit power at S_a. Further, $n_r^I \sim \mathcal{CN}(0, \sigma_r^2)$ and $n_b^I \sim \mathcal{CN}(0, \sigma_b^2)$ are AWGN variables at R and S_b, respectively.

The first fraction $\sqrt{\rho} y_{a,r}^I$ is used for harvesting energy and the second fraction $\sqrt{(1-\rho)} y_{a,r}^I$ is allocated for information transmission.

The harvested energy at relay node in first phase can be given as

$$E_h^I = \frac{\eta\rho P_a |h_{a,r}|^2 T}{3}, \tag{3.20}$$

where $0 < \eta < 1$ represents the energy conversion efficiency.

In second phase, source node S_b transmits unit energy symbol x_b to the nodes R and S_a. Consequently, the received signals at R and S_a can be expressed, respectively, as

$$y_{b,r}^{II} = \sqrt{P_b} h_{b,r} x_b + n_r^{II} \tag{3.21}$$

and

$$y_{b,a}^{II} = \sqrt{P_b} h_{b,a} x_b + n_a^{II}, \tag{3.22}$$

where P_b denotes transmit power at S_b, $n_r^{II} \sim \mathcal{CN}(0, \sigma_r^2)$ and $n_a^{II} \sim \mathcal{CN}(0, \sigma_a^2)$ represent AWGN variables at R and S_a, respectively.

Similar to the first phase, the harvested energy at relay node in second phase can be given as

$$E_h^{II} = \frac{\eta\rho P_b |h_{b,r}|^2 T}{3}. \tag{3.23}$$

Thus, the total harvested energy can be expressed as

$$E_h = \frac{\eta\rho (P_a |h_{a,r}|^2 + P_b |h_{b,r}|^2) T}{3}. \tag{3.24}$$

Amplify-and-Forward (AF): We discussed in detail about AF relaying protocol in Section 2.1.1. Hereby, we have adopted an AF relaying protocol since using DF protocol may increase the chance of error in decoding. This error in decoding is primarily caused because of low power assignment at information decoding circuitry due to power splitting.

In the third IP phase, the AF relay node combines the signals $\sqrt{(1-\rho)} y_{a,r}^I$ and

$\sqrt{(1-\rho)}y_{b,r}^{II}$ and broadcasts the combined signal using AF operation with gain

$$\mathcal{G} \approx 1/\sqrt{(1-\rho)(P_a|h_{a,r}|^2 + P_b|h_{b,r}|^2)}. \tag{3.25}$$

The received signals at the source nodes in third phase can be expressed as

$$y_{r,i}^{III} = \mathcal{G}\sqrt{P_r}h_{r,i}(\sqrt{(1-\rho)}y_{a,r}^{I} + \sqrt{(1-\rho)}y_{b,r}^{II} + n_{cr}^{I} + n_{cr}^{II}) + n_i^{III}, \tag{3.26}$$

where $P_r = \eta\rho(P_a|h_{a,r}|^2 + P_b|h_{b,r}|^2)$ is transmit power at R, $n_{cr} \sim \mathcal{CN}(0, \sigma_{cr}^2)$ denotes RF to baseband conversion noise, and $n_i^{III} \sim \mathcal{CN}(0, \sigma_i^2)$ is AWGN variable at S_i, for $i \in \{a, b\}$.

SNR Analysis

As both S_a and S_b have knowledge about their own information signals, therefore, they can cancel their self-interference. After canceling self-interference and performing MRC with direct link, the instantaneous end-to-end SNR for transmission from $S_\jmath$ to S_i can be expressed as

$$\gamma_{\jmath,i} = \frac{P_\jmath|h_{\jmath,i}|^2}{\sigma_i^2} + \frac{\eta\rho(1-\rho)P_\jmath|h_{r,i}|^2|h_{\jmath,r}|^2}{2\eta\rho((1-\rho)\sigma_r^2 + \sigma_{cr}^2)|h_{r,i}|^2 + (1-\rho)\sigma_i^2}, \tag{3.27}$$

for $i, \jmath \in \{a, b\}$, with $i \neq \jmath$.

Equation (3.27) is used for the outage probability analysis in next chapter for MRC diversity combining technique.

Chapter 4

System Performance Analysis with SC and MRC Schemes

In this chapter, we examine the outage performance of the TWR network with EH at the relay. Apart from communication via relay link, transmission over the direct link is also considered, which improves the link reliability of the system. Firstly, we derive the expression of OP for the SWIPT-enabled bidirectional half-duplex relay network for both SC and MRC diversity combining techniques over Nakagami-m fading channels. After that, by using the expression of the OP, we formulate the expression of system throughput and energy-efficiency for the system, as considered in Chapter 3.

4.1 Selection Combining (SC) Scheme

We have discussed SC scheme in Section 2.2.1 in more detail. Hereby, we derive the expressions of OP, system throughput, and energy-efficiency for hybrid relaying protocols employing the TS-based EH approach.

4.1.1 Outage Probability (OP) Analysis

For a delay-limited transmission, the OP is considered as a crucial performance metric, which defines the probability of link failure [11]. In the considered hybrid TWR scheme, an outage event occurs at the destination node if the corresponding instantaneous data

rate fails to achieve a particular threshold by utilizing both intended signals (direct and relayed). Thereby, the user OP at S_i for the considered set-up can be defined as

$$\begin{aligned}\mathcal{P}_{\text{out},i} = &(1-\Pr[\mathcal{Q}_a])\ (1-\Pr[\mathcal{Q}_b])\Pr[\mathcal{R}_{sc,i}^{\text{AF}} < r_{\text{th}}]\Pr[\mathcal{Q}_a]\ (1-\Pr[\mathcal{Q}_b])\ \Pr[\mathcal{R}_{sc,i}^{\text{AF}} < r_{\text{th}}] \\ &+ (1-\Pr[\mathcal{Q}_a])\ \Pr[\mathcal{Q}_b]\Pr[\mathcal{R}_{sc,i}^{\text{AF}} < r_{\text{th}}]\Pr[\mathcal{Q}_a]\Pr[\mathcal{Q}_b]\Pr[\mathcal{R}_{sc,i}^{\text{DF}} < r_{\text{th}}], \end{aligned} \tag{4.1}$$

where $\Pr[\mathcal{Q}_i]$, for $i \in \{a,b\}$, denotes the probability of decoding of x_a and x_b in the first and second IP phases at R. In (4.1), the first term appears for the case when R fails to decode both signals (x_a and x_b), whereas the second and third terms enlighten the cases when only one signal is decoded successfully. On the other hand, the last term represents the case when R successfully decodes both the signals. Here, we define r_{th} as the predefined target rate for both source nodes. As the SC scheme is employed at both destination nodes to select the best signal corresponding to maximum SNR, the instantaneous data rate can be given as

$$\mathcal{R}_{sc,i}^{k} = \frac{(1-\alpha)}{3}\log_2\left(1+\max\left(\gamma_{r,i}^{k},\gamma_{\jmath,i}\right)\right), \tag{4.2}$$

for $i,\jmath \in \{a,b\}$, with $i \neq \jmath$ and $k \in \{\text{AF},\text{DF}\}$. Now, we derive the required probabilities for obtaining the OP expression defined in (4.1).

First, the $\mathcal{P}_{sc,i}^{\text{AF}} \triangleq \Pr[\mathcal{R}_{sc,i}^{\text{AF}} < r_{\text{th}}]$ can be defined as

$$\begin{aligned}\mathcal{P}_{sc,i}^{\text{AF}} &= \Pr\left[\max\left(\gamma_{r,i}^{\text{AF}},\gamma_{\jmath,i}\right) < \gamma_{\text{th}}\right] \\ &= \Pr\left[\gamma_{r,i}^{\text{AF}} < \gamma_{\text{th}}\right]\Pr\left[\gamma_{\jmath,i} < \gamma_{\text{th}}\right], \end{aligned} \tag{4.3}$$

where $\gamma_{\text{th}} = 2^{\frac{3r_{\text{th}}}{1-\alpha}} - 1$.

CDF Evaluation for AF Relaying

From the definition of CDF, we have

$$F_{\gamma_{r,i}^{\text{AF}}}(\gamma_{\text{th}}) \triangleq \Pr\left[\gamma_{r,i}^{\text{AF}} < \gamma_{\text{th}}\right], \tag{4.4}$$

where $\gamma_{r,i}^{\text{AF}}$ is defined in equation (3.17). Let $X \triangleq |h_{r,i}|^2$ and $Y \triangleq |h_{r,\jmath}|^2$, for $i, \jmath \in \{a, b\}$ with $i \neq \jmath$.

As we consider Nakagami-m fading, therefore, X and Y follow gamma distribution with their respective PDFs as

$$f_X(x) = \left(\frac{m_i}{\Omega_i}\right)^{m_i} \frac{x^{m_i-1}}{\Gamma[m_i]} e^{-\frac{m_i x}{\Omega_i}},\ x \geq 0 \tag{4.5}$$

$$\text{and} \qquad f_Y(y) = \left(\frac{m_\jmath}{\Omega_\jmath}\right)^{m_\jmath} \frac{y^{m_\jmath-1}}{\Gamma[m_\jmath]} e^{-\frac{m_\jmath y}{\Omega_\jmath}},\ y \geq 0. \tag{4.6}$$

The CDF $F_{\gamma_{r,i}^{\text{AF}}}(\gamma_{\text{th}})$ can be expressed using (3.17) as

$$\begin{aligned} F_{\gamma_{r,i}^{\text{AF}}}(\gamma_{\text{th}}) &= \Pr\left[\frac{\xi_i |h_{r,i}|^2 |h_{\jmath,r}|^2}{2|h_{r,i}|^2 + \omega_i} < \gamma_{\text{th}}\right] \\ &= \Pr\left[X < \frac{\omega_i \gamma_{\text{th}}}{\xi_i Y - 2\gamma_{\text{th}}}\right]. \end{aligned} \tag{4.7}$$

From (4.7), the expression of $F_{\gamma_{r,i}^{\text{AF}}}(\gamma_{\text{th}})$ can be formulated in an integral form as

$$F_{\gamma_{r,i}^{\text{AF}}}(\gamma_{\text{th}}) = \underbrace{\int_0^{\frac{2\gamma_{\text{th}}}{\xi_i}} f_Y(y) dy}_{I_1} + \underbrace{\int_{\frac{2\gamma_{\text{th}}}{\xi_i}}^{\infty} f_Y(y) \int_0^{\frac{\omega_i \gamma_{\text{th}}}{\xi_i y - 2\gamma_{\text{th}}}} f_X(x) dx dy}_{I_2}. \tag{4.8}$$

Averaging the PDF of y given in equation (4.6) gives the CDF of the random variable y, which is represented by I_1 as

$$I_1 = \int_0^{\frac{2\gamma_{\text{th}}}{\xi_i}} \left(\frac{m_\jmath}{\Omega_\jmath}\right)^{m_\jmath} \frac{y^{m_\jmath-1}}{\Gamma[m_\jmath]} e^{-\frac{m_\jmath y}{\Omega_\jmath}} dy = \frac{1}{\Gamma}[m_\jmath] \Upsilon\left(m_\jmath, \frac{2\gamma_{\text{th}} m_\jmath}{\xi_i \Omega_\jmath}\right). \tag{4.9}$$

After putting the PDF of the R.V. x and y, we calculate the integral I_2 as

$$I_2 = \int_{\frac{2\gamma_{\text{th}}}{\xi_i}}^{\infty} \left(\frac{m_\jmath}{\Omega_\jmath}\right)^{m_\jmath} \frac{y^{m_\jmath-1}}{\Gamma[m_\jmath]} e^{-\frac{m_\jmath y}{\Omega_\jmath}} \int_0^{\frac{\omega_i \gamma_{\text{th}}}{\xi_i y - 2\gamma_{\text{th}}}} \left(\frac{m_i}{\Omega_i}\right)^{m_i} \frac{x^{m_i-1}}{\Gamma[m_i]} e^{-\frac{m_i x}{\Omega_i}} dx dy. \tag{4.10}$$

By applying the method of change of variable and using the gamma function as $\Upsilon(n, w) = \int_0^w t^{n-1} e^{-t} dt$.

Further, simplify the equation (4.10) as

$$I_2 = \frac{1}{\Gamma[m_\jmath]\Gamma[m_i]} \left(\frac{m_\jmath}{\Omega_\jmath}\right)^{m_\jmath} \int_{\frac{2\gamma_{\rm th}}{\xi_i}}^{\infty} y^{m_\jmath - 1} e^{-\frac{m_\jmath y}{\Omega_\jmath}} \Upsilon\left(m_i, \frac{m_i \omega_i \gamma_{\rm th}}{\Omega_i(\xi_i y - 2\gamma_{\rm th})}\right) dy. \tag{4.11}$$

Hereby, we utilize the approximation of gamma function which is given by

$$\Upsilon\left(m, \frac{m}{\Omega}x\right) = \Gamma[m]\left(1 - e^{\frac{m}{\Omega}x} \sum_{k=0}^{\infty} \frac{\left(\frac{m}{\Omega}x\right)^k}{k!}\right) \tag{4.12}$$

Further, we simplify the equation (4.11), after using the approximation of the gamma function, as

$$\begin{aligned} I_2 = &\frac{1}{\Gamma[m_\jmath]} \left(\frac{m_\jmath}{\Omega_\jmath}\right)^{m_\jmath} \left(\left(\frac{\Omega_\jmath}{m_\jmath}\right)^{m_\jmath} \Gamma\left(m_\jmath, \frac{2m_\jmath \gamma_{\rm th}}{\Omega_\jmath \xi_i}\right) - \sum_{k=0}^{m_i - 1} \frac{\left(\frac{m_i \omega_i \gamma_{\rm th}}{\Omega_i}\right)^k}{k!} \right. \\ &\left. \times \underbrace{\int_{\frac{2\gamma_{\rm th}}{\xi_i}}^{\infty} y^{m_\jmath - 1} e^{-\frac{m_\jmath y}{\Omega_\jmath}} e^{-\frac{m_i \omega_i \gamma_{\rm th}}{\Omega_i(\xi_i y - 2\gamma_{\rm th})}} (\xi_i y - 2\gamma_{\rm th})^{-k} dy}_{I_3} \right). \end{aligned} \tag{4.13}$$

By substituting $\xi_i y - 2\gamma_{\rm th} = t$ and solving I_3, we get

$$I_3 = \frac{1}{\xi_i^{m_\jmath}} e^{-\frac{2m_\jmath \gamma_{th}}{\Omega_\jmath \xi_i}} \sum_{q=0}^{m_\jmath - 1} \binom{m_\jmath - 1}{q} (2\gamma_{th})^{(m_\jmath - q - 1)} \int_0^{\infty} t^{(q-k)} e^{-\frac{m_\jmath t}{\Omega_\jmath \xi_i} - \frac{m_i \gamma_{th} \omega_i}{\Omega_i t}} dt. \tag{4.14}$$

After the application of the following integral formula

$$\int_0^{\infty} x^{(v-1)} e^{-\frac{R}{x} - Qx} dx = 2\left(\frac{R}{Q}\right)^{\left(\frac{v}{2}\right)} K_v\left(2\sqrt{RQ}\right),$$

we obtain

$$I_3 = \frac{1}{\xi_i^{m_\jmath}} e^{-\frac{2m_\jmath \gamma_{th}}{\Omega_\jmath \xi_i}} \sum_{q=0}^{m_\jmath - 1} \binom{m_\jmath - 1}{q} (2\gamma_{th})^{(m_\jmath - q - 1)} 2\left(\frac{m_i \Omega_\jmath \gamma_{th} \omega_i \xi_i}{m_\jmath \Omega_i}\right)^{\frac{q-k+1}{2}} K_v\left(2\sqrt{\frac{m_i m_\jmath \gamma_{th} \omega_i}{\xi_i \Omega_i \Omega_\jmath}}\right), \tag{4.15}$$

where v=q-k+1 and K_v is the v^{th} order bessel function which is defined in [34, eq.

(8.432.1)].

By using the equation (4.8),(4.9),(4.13), and (4.15), we express the CDF of the relay link at the destination as

$$F_{\gamma_{r,i}^{\mathrm{AF}}}(\gamma_{\mathrm{th}}) = 1 - \frac{1}{\Gamma[m_\jmath]}\left(\frac{m_\jmath}{\Omega_\jmath}\right)^{m_\jmath}\sum_{k=0}^{m_i-1}\sum_{q=0}^{m_\jmath-1}\frac{\left(\frac{m_i\omega_i}{\Omega_i}\right)^k}{\xi_i^{m_\jmath}k!}2^{m_\jmath-q}\binom{m_\jmath-1}{q}\left(\frac{\xi_i m_i\Omega_\jmath\omega_i}{m_\jmath\Omega_i}\right)^{\frac{q-k+1}{2}}$$
$$\times\,\gamma_{th}^{\frac{2m_\jmath+k-q-1}{2}}e^{-\frac{2m_\jmath\gamma_{\mathrm{th}}}{\Omega_\jmath\xi_i}}\mathcal{K}_{q-k+1}\left(2\sqrt{\frac{m_i m_\jmath\omega_i\gamma_{\mathrm{th}}}{\xi_i\Omega_i\Omega_\jmath}}\right). \tag{4.16}$$

Now, the probability of last term of (4.1), i.e., $\mathcal{P}_{sc,i}^{\mathrm{DF}} \triangleq \Pr[\mathcal{R}_{sc,i}^{\mathrm{DF}} < r_{\mathrm{th}}]$ can be defined as

$$\begin{aligned}\mathcal{P}_{sc,i}^{\mathrm{DF}} &= \Pr\left[\max\left(\gamma_{r,i}^{\mathrm{DF}},\gamma_{\jmath,i}\right) < \gamma_{\mathrm{th}}\right]\\ &= \Pr\left[\gamma_{r,i}^{\mathrm{DF}} < \gamma_{\mathrm{th}}\right]\Pr\left[\gamma_{\jmath,i} < \gamma_{\mathrm{th}}\right].\end{aligned} \tag{4.17}$$

CDF Evaluation for DF Relaying

From the definition of the CDF, we can express
$F_{\gamma_{r,i}^{\mathrm{DF}}}(\gamma_{\mathrm{th}}) \triangleq \Pr\left[\gamma_{r,i}^{\mathrm{DF}} < \gamma_{\mathrm{th}}\right]$,
where γ^{DF} is defined in the equation (3.16). The cdf expression is

$$\begin{aligned}F_{\gamma_{r,i}^{\mathrm{DF}}}(\gamma_{\mathrm{th}}) &= \Pr\left[\frac{(\varepsilon_i X+\varepsilon_\jmath Y)X}{\varphi} < \gamma_{\mathrm{th}}\right]\\ &= \Pr\left[Y < \left(\frac{\gamma_{\mathrm{th}}\varphi}{X\varepsilon_\jmath} - \frac{\varepsilon_i X}{\varepsilon_\jmath}\right)\right].\end{aligned} \tag{4.18}$$

On defining the probability in (4.18) in integral form as

$$F_{\gamma_{r,i}^{\mathrm{DF}}}(\gamma_{\mathrm{th}}) = \int_0^{\sqrt{\frac{\gamma_{\mathrm{th}}\varphi}{\varepsilon_i}}} f_X(x)\int_0^{\frac{\gamma_{\mathrm{th}}\varphi}{x\varepsilon_\jmath}-\frac{\varepsilon_i x}{\varepsilon_\jmath}} f_Y(y)dy\,dx. \tag{4.19}$$

By using the PDFs of X and Y in (4.19), we represent it as

$$F_{\gamma_{r,i}^{\mathrm{DF}}}(\gamma_{\mathrm{th}}) = \frac{1}{\Gamma[m_i]}\Upsilon\left[m_i, \frac{m_i\phi_i}{\Omega_i}\right] - \frac{1}{\Gamma[m_i]}\left(\frac{m_i}{\Omega_i}\right)^{m_i}\sum_{l=0}^{m_\jmath-1}\frac{1}{l!}\left(\frac{m_\jmath}{\Omega_\jmath}\right)^{l}\sum_{p=0}^{l}\binom{l}{p}\left(\frac{\gamma_{\mathrm{th}}\varphi}{\varepsilon_\jmath}\right)^{p} \times \left(-\frac{\varepsilon_i}{\varepsilon_\jmath}\right)^{l-p}\int_0^{\phi_i} x^{l+m_i-2p-1}e^{-\frac{m_\jmath\gamma_{\mathrm{th}}\varphi}{\Omega_\jmath\varepsilon_\jmath x}-\left(\frac{m_i}{\Omega_i}-\frac{\varepsilon_i m_\jmath}{\varepsilon_\jmath\Omega_\jmath}\right)x}dx. \tag{4.20}$$

For evaluating (4.20), we consider two cases i.e., $\frac{m_i}{\Omega_i} = \frac{\varepsilon_i m_\jmath}{\varepsilon_\jmath\Omega_\jmath}$ and $\frac{m_i}{\Omega_i} \neq \frac{\varepsilon_i m_\jmath}{\varepsilon_\jmath\Omega_\jmath}$.

The CDF $F_{\gamma_{r,i}^{\mathrm{DF}}}(\gamma_{\mathrm{th}})$ can be expressed as

$$F_{\gamma_{r,i}^{\mathrm{DF}}}(\gamma_{\mathrm{th}}) = \begin{cases} \mathcal{P}_{DF_i} & \text{for } \frac{m_\jmath\varepsilon_i}{\Omega_\jmath\varepsilon_\jmath} = \frac{m_i}{\Omega_i}, \\ \widetilde{\mathcal{P}}_{DF_i} & \text{for } \frac{m_\jmath\varepsilon_i}{\Omega_\jmath\varepsilon_\jmath} \neq \frac{m_i}{\Omega_i}, \end{cases} \tag{4.21}$$

by utilizing the fact [34, eq. 3.381.6], the final solution for these cases are given as

$$\mathcal{P}_{DF_i} = \frac{1}{\Gamma[m_i]}\Upsilon\left[m_i, \frac{m_i\phi_i}{\Omega_i}\right] - \left(\frac{m_i}{\Omega_i}\right)^{m_i}\sum_{l=0}^{m_\jmath-1}\frac{\left(\frac{m_\jmath}{\Omega_\jmath}\right)^{l}}{l!}\sum_{p=0}^{l}\binom{l}{p}\left(\frac{\gamma_{\mathrm{th}}\varphi}{\varepsilon_\jmath}\right)^{p}\left(\frac{-\varepsilon_i}{\varepsilon_\jmath}\right)^{l-p} \times \left(\frac{m_\jmath\gamma_{\mathrm{th}}\varphi}{\Omega_\jmath\varepsilon_\jmath}\right)^{l+m_i-2p}\frac{1}{\Gamma[m_i]}\left(\frac{m_\jmath\gamma_{\mathrm{th}}\varphi}{\Omega_\jmath\varepsilon_\jmath\phi_i}\right)^{-\frac{(l+m_i-2p+1)}{2}} e^{-\left(\frac{m_\jmath\gamma_{\mathrm{th}}\varphi}{2\Omega_\jmath\varepsilon_\jmath\phi_i}\right)} \times \mathcal{W}_{-\frac{(l+m_i-2p+1)}{2},\frac{1-(l+m_i-2p+1)}{2}}\left(\frac{m_\jmath\gamma_{\mathrm{th}}\varphi}{\Omega_\jmath\varepsilon_\jmath\phi_i}\right) \tag{4.22}$$

and

$$\widetilde{\mathcal{P}}_{DF_i} = \frac{1}{\Gamma[m_i]}\Upsilon\left[m_i, \frac{m_i\phi_i}{\Omega_i}\right] - \frac{1}{\Gamma[m_i]}\left(\frac{m_i}{\Omega_i}\right)^{m_i}\sum_{l=0}^{m_\jmath-1}\frac{\left(\frac{m_\jmath}{\Omega_\jmath}\right)^{l}}{l!}\sum_{p=0}^{l}\sum_{k=0}^{\infty}\binom{l}{p}\left(\frac{\gamma_{\mathrm{th}}\varphi}{\varepsilon_\jmath}\right)^{p} \times \left(\frac{-\varepsilon_i}{\varepsilon_\jmath}\right)^{l-p}\frac{\left(\frac{\varepsilon_i m_\jmath}{\varepsilon_\jmath\Omega_\jmath}-\frac{m_i}{\Omega_i}\right)^{k}}{k!}\left(\frac{m_\jmath\gamma_{\mathrm{th}}\varphi}{\Omega_\jmath\varepsilon_\jmath}\right)^{l+m_i+k-2p}\left(\frac{m_\jmath\gamma_{\mathrm{th}}\varphi}{\Omega_\jmath\varepsilon_\jmath\phi_i}\right)^{-\frac{(l+m_i+k-2p+1)}{2}} e^{-\left(\frac{m_\jmath\gamma_{\mathrm{th}}\varphi}{2\Omega_\jmath\varepsilon_\jmath\phi_i}\right)} \times \mathcal{W}_{-\frac{(l+m_i+k-2p+1)}{2},\frac{1-(l+m_i+k-2p+1)}{2}}\left(\frac{m_\jmath\gamma_{\mathrm{th}}\varphi}{\Omega_\jmath\varepsilon_\jmath\phi_i}\right). \tag{4.23}$$

Other probability term of (4.3), i.e., $F_{\gamma_{\jmath,i}}(\gamma_{\rm th}) \triangleq \Pr[\gamma_{\jmath,i} < \gamma_{\rm th}]$, can be expressed as,

$$F_{\gamma_{\jmath,i}}(\gamma_{\rm th}) = \Pr\left[|h_{\jmath,i}|^2 < \frac{\gamma_{\rm th}\sigma_i^2}{P_\jmath}\right] = \frac{1}{\Gamma[m_d]}\Upsilon\left[m_d, \frac{m_d\gamma_{\rm th}\sigma_i^2}{\Omega_d P_\jmath}\right]. \tag{4.24}$$

Further, we obtain the expressions of decoding probabilities of both signals (x_a and x_b) at relay node, by using the SNR equations (3.14) and (3.15), as

$$\Pr[\mathcal{Q}_i] = \Pr\left[\gamma_{i,r} \geq \gamma_{\rm th}\right] = \frac{1}{\Gamma[m_i]}\Gamma\left[m_i, \frac{m_i\gamma_{\rm th}\sigma_r^2}{\Omega_i P_i}\right]. \tag{4.25}$$

4.1.2 System Throughput

Throughput for the considered SWIPT-enabled TWR system can be defined as the sum of average target rates of both source nodes that can be successfully achieved over fading channels. Moreover, it is also referred to as mean spectral efficiency of the relay based wireless system. By using the derived expressions of OP, we can define it as

$$\mathcal{S}_\mathcal{T} = \frac{(1-\alpha)}{3}\big[(1-\mathcal{P}_{{\rm out},a})r_{\rm th} + (1-\mathcal{P}_{{\rm out},b})r_{\rm th}\big], \tag{4.26}$$

where $\mathcal{P}_{{\rm out},a}$ and $\mathcal{P}_{{\rm out},b}$ are OP of the $S_b \to S_a$ and $S_a \to S_b$ links, respectively.

4.2 Maximum-Ratio Combining (MRC) Scheme

We have discussed MRC in Section 2.2.2 in detail. Here, we use that with detailed mathematical description. More specifically, we derive the various performance matrices, as discussed earlier for AF relaying protocol employing the PS-based approach for the EH purpose.

4.2.1 OP Analysis

OP is considered as a key performance parameter for the delay-limited wireless system, which defines the probability of link failure. In the considered system, an outage event takes place at the receiving node if the corresponding instantaneous data rate falls below

a particular target rate. Therefore, the expression of user OP at S_i can be formulated as

$$\mathcal{P}_{\text{out},i} = \Pr[\gamma_{\jmath,i} < \gamma_{\text{th}}] = \Pr\left[\omega_i |h_{\jmath,i}|^2 + \frac{\xi_i |h_{r,i}|^2 |h_{\jmath,r}|^2}{\beta |h_{r,i}|^2 + \mu_i} < \gamma_{\text{th}}\right], \tag{4.27}$$

where $\gamma_{\jmath,i}$ is defined in equation (3.27), $\omega_i = P_\jmath/\sigma_i^2$, $\beta = 2\eta\rho((1-\rho)\sigma_r^2 + \sigma_{cr}^2)$, $\xi_i = \eta\rho(1-\rho)P_\jmath$, $\mu_i = (1-\rho)\sigma_i^2$, and $\gamma_{\text{th}} = 2^{3r_{\text{th}}} - 1$.

Let $X \triangleq |h_{r,i}|^2$, $Y \triangleq |h_{r,\jmath}|^2$, and $Z \triangleq |h_{\jmath,i}|^2$, for $i, \jmath \in \{a, b\}$ with $i \neq \jmath$. We assume Nakagami-m fading scenario, therefore, X, Y, and Z will follow gamma distribution. The outage probability expression (4.27) can be defined as

$$\mathcal{P}_{\text{out},i} = \Pr\left[\omega_i Z + \frac{\xi_i XY}{\beta X + \mu_i} < \gamma_{\text{th}}\right], \tag{4.28}$$

which can be further expressed in an integral form as

$$\mathcal{P}_{\text{out},i} = \int_0^{\frac{\gamma_{\text{th}}}{\omega_i}} F_V(\varphi_i) f_Z(z) dz, \tag{4.29}$$

where $V = \frac{\xi_i XY}{\beta X + \mu_i}$ and $\varphi_i = \gamma_{\text{th}} - \omega_i z$.

For deriving (4.29), we first obtain the CDF $F_V(\varphi_i)$.

CDF Evalution

$$\begin{aligned} F_V(\varphi_i) &= \Pr\left[\frac{\xi_i XY}{\beta X + \mu_i} < \varphi_i\right] \\ &= \int_{\frac{\beta\varphi_i}{\xi_i}}^{\infty} f_Y(y) \int_0^{\theta} f_X(x) dx\, dy + \int_0^{\frac{\beta\varphi_i}{\xi_i}} f_Y(y) dy, \end{aligned} \tag{4.30}$$

where $\theta = \frac{\varphi_i \mu_i}{\xi_i y - \beta\varphi_i}$.

After some mathematical formulations and utilizing the fact [34, eq. 3.471.9], we obtain

$$F_V(\varphi_i) = 1 - \frac{1}{\Gamma[m_\jmath]} \left(\frac{m_\jmath}{\Omega_\jmath}\right)^{m_\jmath} \sum_{k=0}^{m_i-1} \mu_i^k \sum_{p=0}^{m_\jmath-1} \varphi_i^{k+p} \frac{\beta^p}{\xi_i^{m_\jmath}} 2\binom{m_\jmath-1}{p} \frac{\left(\frac{m_i}{\Omega_i}\right)^k}{k!}$$
$$\times e^{-\frac{m_\jmath \beta \varphi_i}{\xi_i \Omega_\jmath}} \left(\frac{m_i \Omega_\jmath \xi_i \mu_i \varphi_i}{\Omega_i m_\jmath}\right)^{\frac{m_\jmath-k-p}{2}} \mathcal{K}_{m_\jmath-k-p}\left(2\sqrt{\frac{m_i m_\jmath \mu_i \varphi_i}{\xi_i \Omega_i \Omega_\jmath}}\right). \tag{4.31}$$

After inserting the CDF expression of (4.31) in (4.29) and applying some well known mathematical results, we can express (4.29) as

$$\mathcal{P}_{\text{out},i} = \frac{1}{\Gamma[m_0]} \Upsilon\left(m_0, \frac{m_0 \gamma_{\text{th}}}{\Omega_0 \omega_i}\right) - \frac{1}{\Gamma[m_\jmath]} \left(\frac{m_\jmath}{\Omega_\jmath}\right)^{m_\jmath} \sum_{k=0}^{m_i-1} \sum_{p=0}^{m_\jmath-1} \sum_{l=0}^{\infty} \sum_{q=0}^{\infty} \sum_{r=0}^{m_0+l-1} \frac{\left(\frac{m_i}{\Omega_i}\right)^k}{k!}$$
$$\times \frac{2}{\Gamma[m_\jmath]} \left(\frac{m_0}{\Omega_0}\right)^{m_0} e^{-\left(\frac{m_\jmath \beta \gamma_{\text{th}}}{\xi_i \Omega_\jmath}\right)} \frac{\left(\frac{m_\jmath \beta \omega_i}{\xi_i \Omega_\jmath}\right)^l}{l!} \left(\frac{m_i \Omega_\jmath \xi_i \mu_i}{\Omega_i m_\jmath}\right)^{\frac{m_\jmath-k-p}{2}} \frac{\mu_i^k \beta^p}{\xi_i^{m_\jmath}} \binom{m_\jmath-1}{p}$$
$$\times \left(\frac{1}{\omega_i}\right)^{m_0+l} \frac{\left(\frac{m_0}{\Omega_0 \omega_i}\right)^q}{q!} \binom{m_0+l-1}{r} \gamma_{\text{th}}^{m_0+l-r-1} (-1)^r e^{-\left(\frac{m_0 \gamma_{\text{th}}}{\omega_i \Omega_0}\right)}$$
$$\times \underbrace{\int_0^{\gamma_{\text{th}}} t^{\frac{m_\jmath+p+k+2r+2q}{2}} \mathcal{K}_v\left(2\sqrt{\frac{m_i m_\jmath \mu_i t}{\xi_i \Omega_i \Omega_\jmath}}\right) dt}_{\Xi_{i,v}}, \tag{4.32}$$

where the expression of $\Xi_{i,v}$ can be given as

$$\Xi_{i,v} = \begin{cases} \Xi_{i,\text{nz}} & \text{for } m_\jmath - k - p \neq 0 \\ \Xi_{i,0} & \text{for } m_\jmath - k - p = 0. \end{cases} \tag{4.33}$$

As the direct integration of integral $\Xi_{i,v}$ of (4.32) seems intractable for arbitrary values of $v = m_\jmath - k - p$, we first apply approximation on $\mathcal{K}_v$ using [34, eqs. 8.446, 8.447.3] and then obtain the expressions of $\Xi_{i,\text{nz}}$ and $\Xi_{i,0}$ as given in (4.34) and (4.35), respectively.

$$\Xi_{i,\text{nz}} = \sum_{j=0}^{m_\jmath-p-k-1} \frac{\Gamma[m_\jmath-k-p-j]}{2\Gamma[j+1]} (-1)^j \left(\frac{m_i m_\jmath \mu_i}{\xi_i \Omega_i \Omega_\jmath}\right)^{\frac{2j+k+p-m_\jmath}{2}} \frac{{\gamma_{\text{th}}}^{k+p+r+q+j+1}}{k+p+r+q+j+1} + \sum_{s=0}^{\infty} \frac{(-1)^{m_\jmath-k-p+1}}{\Gamma[s+1]\Gamma[s+m_\jmath-k-p]}$$
$$\times \left(\frac{m_i m_\jmath \mu_i}{\xi_i \Omega_i \Omega_\jmath}\right)^{\frac{m_\jmath-k-p+2s}{2}} \left(\lim_{F\to\infty} \frac{1}{2} \frac{\gamma_{\text{th}}}{F} \sum_{g=1}^{F} \left(\frac{g\gamma_{\text{th}}}{F}\right)^{m_\jmath+r+q+s} \ln\left(\frac{m_i m_\jmath \mu_i g \gamma_{\text{th}}}{\xi_i \Omega_i \Omega_\jmath F}\right)\right.$$
$$\left. - \left(\frac{\Psi[s+1]}{2} + \frac{\Psi[m_\jmath-k-p+s+1]}{2}\right) \frac{(\gamma_{\text{th}})^{m_\jmath+r+q+s+1}}{m_\jmath+r+q+s+1}\right) \tag{4.34}$$

and

$$\Xi_{i,0} = \sum_{j=0}^{\infty} \frac{\left(\frac{m_i m_j \mu_i}{\xi_i \Omega_i \Omega_j}\right)^j}{(j!)^2} \frac{2\Psi[j+1]\gamma_{\text{th}}^{\frac{m_j+k+p+2r+2q+2j+2}{2}}}{m_j+k+p+2r+2q+2j+2} - \frac{1}{2}\sum_{s=0}^{\infty} \frac{\left(\frac{m_i m_j \mu_i}{\xi_i \Omega_i \Omega_j}\right)^s}{(s!)^2} \lim_{n\to\infty}\left(\frac{\gamma_{\text{th}}}{n}\right) \times \sum_{m=1}^{n} \left(\frac{m\gamma_{\text{th}}}{n}\right)^{\frac{m_j+k+p+2r+2q+2s}{2}} \ln\left(\frac{m_i m_j \mu_i m \gamma_{\text{th}}}{\xi_i \Omega_i \Omega_j n}\right). \tag{4.35}$$

4.2.2 System Throughput

System throughput for the considered three-phase TWR system can be defined as the sum of individual target rates at both source nodes that can be achieved successfully over fading channel. On using the derived OP expressions, we can formulate it as

$$\mathcal{S}_{\mathcal{T}} = \frac{1}{3}\big[(1-\mathcal{P}_{\text{out},a})r_{\text{th}} + (1-\mathcal{P}_{\text{out},b})r_{\text{th}}\big], \tag{4.36}$$

where $\mathcal{P}_{\text{out},a}$ and $\mathcal{P}_{\text{out},b}$ represent respective OP expressions of the $S_b \to S_a$ and $S_a \to S_b$ links as presented in equation (4.32).

4.2.3 Energy Efficiency

Analysis of energy efficiency in wireless networks has been paid increasing attention to proceed towards realizing green communication systems. From the classical definition, energy efficiency can be defined as the total amount of data delivered to total amount of consumed energy [25]. For a delay-limited system, the expression of energy efficiency can be given as

$$\eta_{\text{EE}}^{\text{PS}} = \frac{\mathcal{S}_{\mathcal{T}}}{(P_a+P_b)/3} = \frac{r_{\text{th}}\big[(1-\mathcal{P}_{\text{out},a})+(1-\mathcal{P}_{\text{out},b})\big]}{P_a+P_b}, \tag{4.37}$$

where $\mathcal{P}_{\text{out},a}$ and $\mathcal{P}_{\text{out},b}$ represent respective OP expressions of the $S_b \to S_a$ and $S_a \to S_b$ links as presented in equation (4.32) and r_{th} represents the system target rate.

Chapter 5

Numerical and Simulation Results

In this chapter, we present the numerical and simulation results to validate the theoretical analysis of previous chapters. We also demonstrate the effects of key system and channel parameters on the outage probability, system throughput, and energy efficiency for the considered SWIPT-enabled TWR system.

Throughout this section, we set $P_a = P_b = P$, $\sigma_i^2 = \sigma_r^2 = \sigma^2$, and define $\frac{P}{\sigma^2}$ as the SNR. Further, we adopt a linear relaying model, where the distance between S_a to S_b is considered to be unity and a relay node is placed at a distance d from source node S_a. We consider the normalized distances $d_a = d$ for $S_a \to R$ link and $d_b = (1-d)$ for $S_b \to R$ link. By adopting the path-loss model, we define $\Omega_a = d^{-3}$ and $\Omega_b = (1-d)^{-3}$ with exponent $\nu = 3$.

5.1 Hybrid Relaying with SC

This section demonstrates the analytical results for TS protocol which provide the insights into various design parameters.

For numerical investigations in Fig. 5.1, we set $\eta = 0.9$, $\alpha = 0.2$, and $r_{\text{th}} = 1$ bps/Hz. Herein, we plot the OP versus SNR curves for the considered system and compare the OP performance of proposed SWIPT-HDAF scheme with other similar schemes, e.g., SWIPT-AF and SWIPT-DF. All the analytical curves in this figure are obtained using (4.1)-(4.23) by truncating the infinite series up to first seven terms to

get the sufficient accuracy. To highlight the need of relaying with SWIPT, we compare the OP performance of the considered system with the direct link (without SWIPT and relaying). From Fig. 5.1, one can observe that the considered scheme outperforms the other three schemes for entire SNR range. The OP performance of SWIPT-AF and SWIPT-DF is somewhat identical. However, they show better performance than that of the direct link for medium and higher SNR values. As expected, when the value of m_a increases from 1 to 2, the system exhibits better OP performance. Consequently, one can infer that the system outage performance improves for higher values of fading severity parameters.

For obtaining numerical results in Fig. 5.2, we set fading severity parameters $m_a = m_b = 2, m_d = 1$, and $r_{\text{th}} = 1$ bps/Hz. In Fig. 5.2, we plot OP versus SNR curves for different values of TS factor α and energy conversion efficiency η. From Fig. 5.2, one can readily observe that when the value of α increases, the OP performance degrades significantly at lower to medium SNR range. This OP behavior is reflected due to the fact that the value of target SNR $\gamma_{\text{th}} = 2^{\frac{3r_{\text{th}}}{1-\alpha}} - 1$ directly depends on the value of α. The higher value of α reflects higher target SNR value. Different from the behavior of α, when the value of η increases, the corresponding OP performance improves. This is quite obvious because it affects the amount of harvested energy during the EH phase.

In Fig. 5.3, we plot the throughput versus SNR curves for various fading severity parameters and target rates. For this, we set $\alpha = 0.2$ and $\eta = 0.9$. From Fig. 5.3, one can manifestly see that when the value of SNR increases, the system throughput increases up to a certain value of SNR and after that it attains a saturated value. This saturated value is referred to as the maximum achievable throughput for a particular target rate. As such, the system throughput for higher target rates attains saturation point at relatively higher SNR values. This is due to the fact that for a fixed SNR, OP corresponding to higher target rate shows poor performance than that of the lower target rate.

In Figs. 5.1 - 5.3, all the analytical curves are in well agreements with the simulation results, which verify the accuracy of our derived expressions.

Fig. 5.4 demonstrates the joint impact of target rate r_{th} and TS factor α on the

system throughput. Herein, we set $\eta = 0.9$, SNR = 10 dB, $m_a = m_b = 2$, and $m_d = 1$. From this figure, one can observe that, at a fixed SNR, the system achieves maximum throughput at a certain target rate only (say r_{th}^*). If the target rate increases or decreases from that value, throughput starts falling towards its minimum value. One can also note that α significantly affects the value of r_{th}^*. When the value of α increases, the value of r_{th}, for which system attain maximum throughput, decreases.

5.2 AF Relaying with MRC

This section introduces the analytical results for PSR protocol which provide the insights into various design choices.

For numerical investigation in Fig. 5.5, we set $\eta = 0.9$, $\rho = 0.5$, and $r_{\text{th}} = 1$ bps/Hz. In this figure, we plot the OP versus SNR curves for the considered system and compare the OP performance with a competitive scheme i.e., two-phase two-way relaying with SWIPT. We utilize (4.27)-(4.35) to obtain all the analytical curves by truncating the infinite series up to first twenty terms to get the required accuracy. We also compare the OP performance of the considered system with the only direct link scheme to highlight the importance of energy harvesting and relaying. From Fig. 5.5, one can readily note that the considered three-phase scheme outperforms two-phase scheme in mid-to-high SNR region. At lower SNR values, two-phase scheme shows slightly better OP performance than that of the considered scheme because it requires less number of phases. In fact, the required target SNR for two-phase scheme will be lesser i.e., $2^{2r_{\text{th}}} - 1$ as compared to three-phase scheme i.e., $2^{3r_{\text{th}}} - 1$. At higher SNR values, due to exploitation of direct link, considered scheme shows better performance than the counterpart. However, the OP performance of SWIPT-based relaying schemes are better than that of the direct link only scheme for entire SNR region. As such, when the value of fading severity parameters increases from 1 to 2, the system depicts better OP performance. From this, one can infer that the exploitation of the MRC with direct link can significantly improve the system's OP performance.

In Fig. 5.6, we plot OP curves versus power splitting factor ρ for different values

of fading severity parameter and target rate. Herein, we set SNR = 15 dB, $d = 0.6$, and $\eta = 0.9$. From this figure, one can observe the valley nature of OP performance with respect to ρ, where system attains higher OP at lower and higher values of ρ. At medium values, OP performance seems to be flat. This OP behavior is reflected due to the presence of direct link. On the other hand, the OP curves corresponding to higher values of target rate shows higher OP. From Figs. 5.5 and 5.6, one can readily see that all the analytical curves are in good consonance with the simulation results, which verify the accuracy of our mathematical framework.

Fig. 5.7 demonstrates the joint effect of SNR and target rate r_{th} on the energy efficiency of the considered system. Herein, we set $\eta = 0.9$, $m_a = 1, m_b = 2, m_0 = 2$, and $\rho = 0.5$. From this figure, one can observe that the system achieves maximum energy efficiency at a certain SNR value only for a fixed target rate. If the target rate changes from that value, the SNR value for which system attains maximum energy efficiency also changes. One can also note that energy efficiency of the considered system is lowest at higher SNR region. This is due to fact that for higher SNR values, the consumed power is much higher than the achieved system throughput.

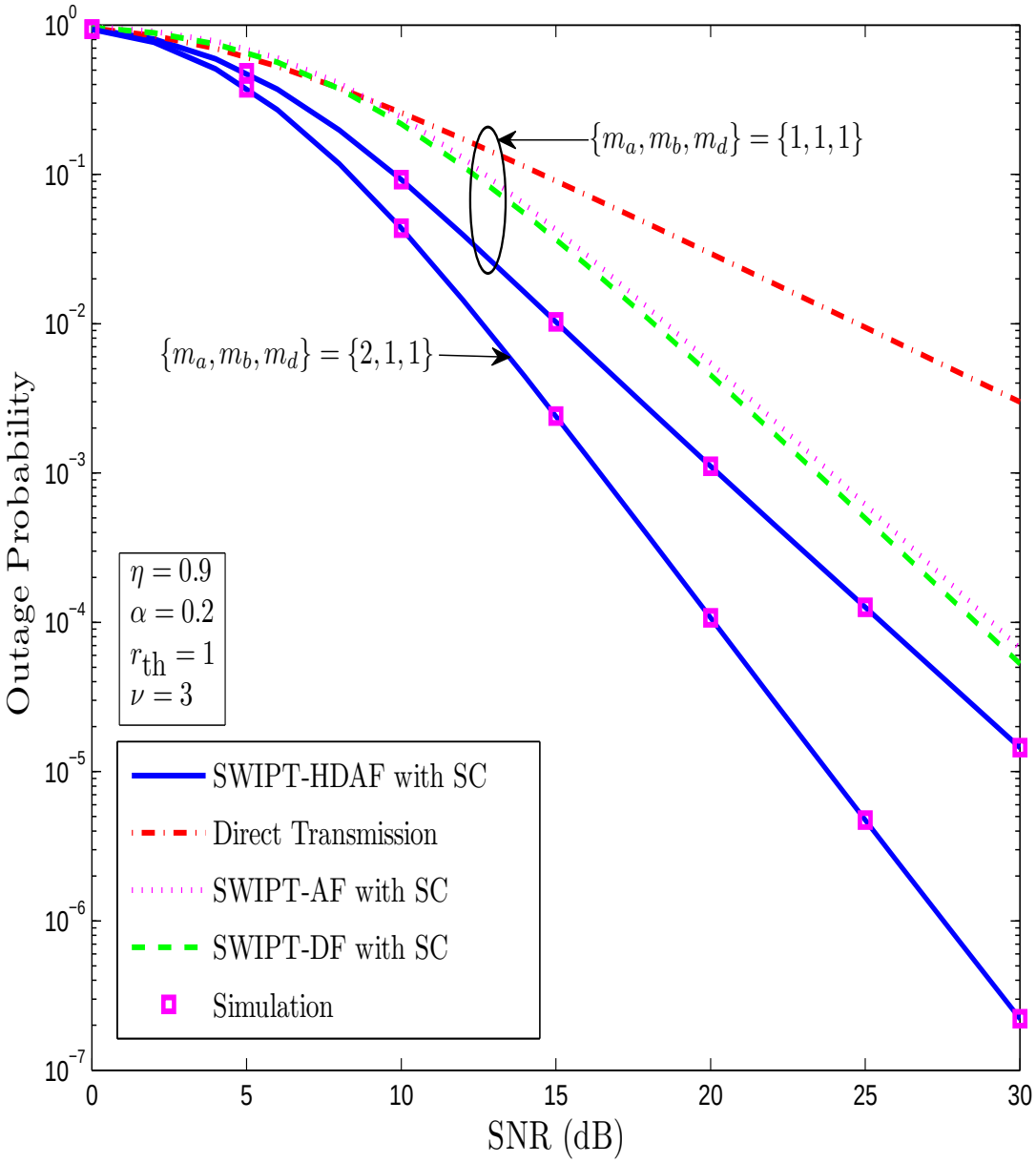

Figure 5.1: OP versus SNR curves for $S_b \to S_a$ link with various schemes.

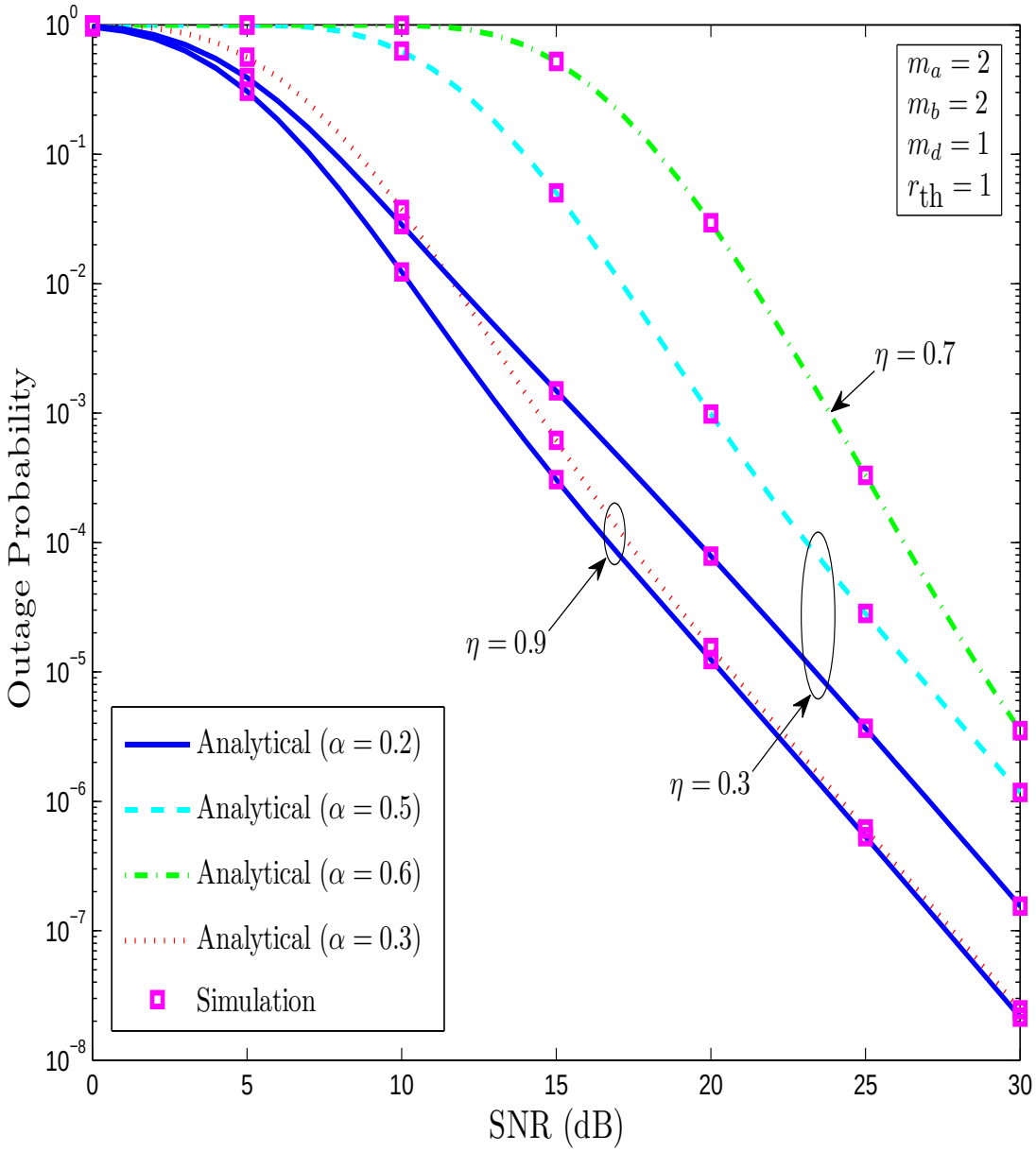

Figure 5.2: OP versus SNR curves for $S_b \to S_a$ link with different parameters.

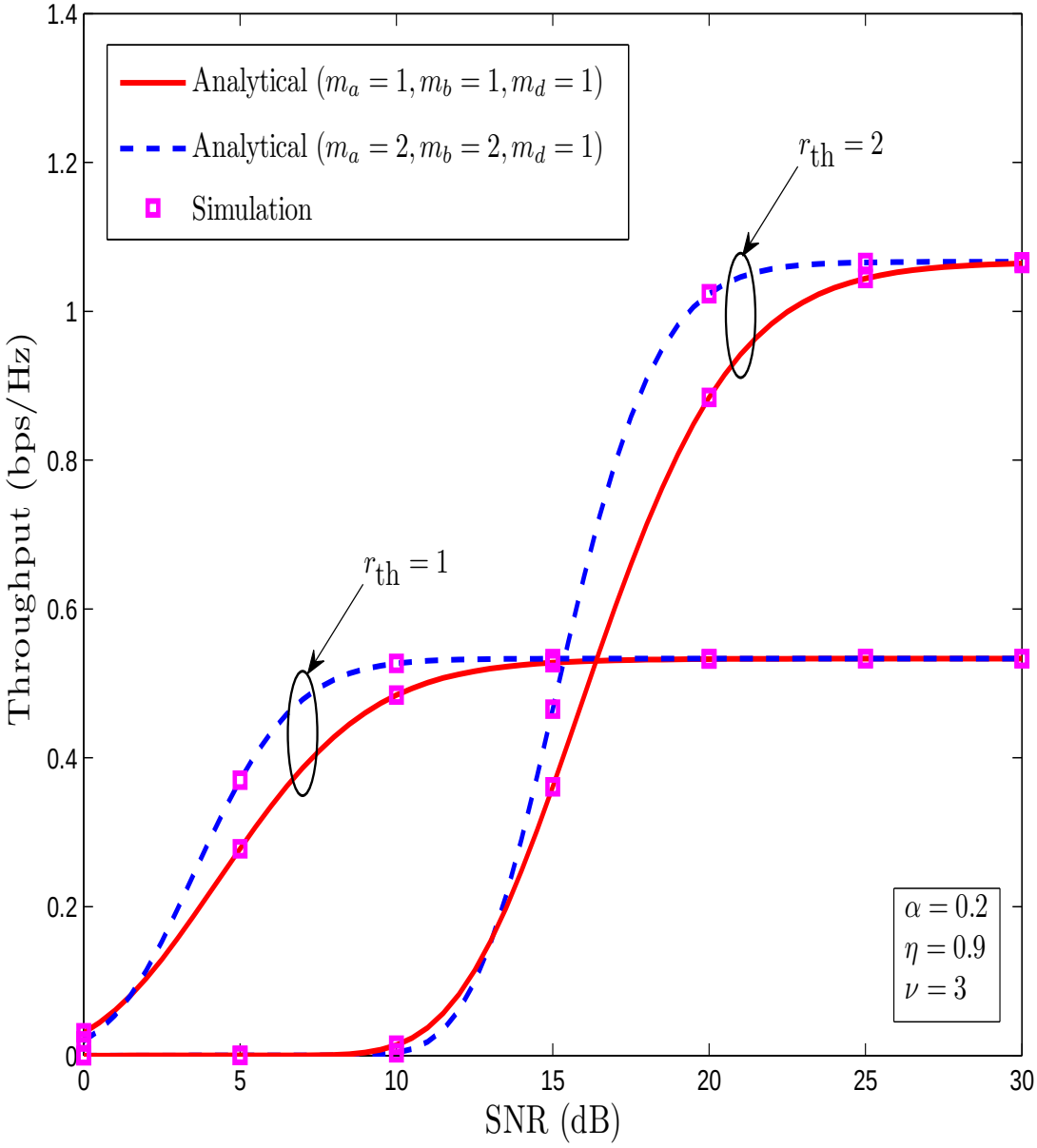

Figure 5.3: Throughput versus SNR curves with different parameters.

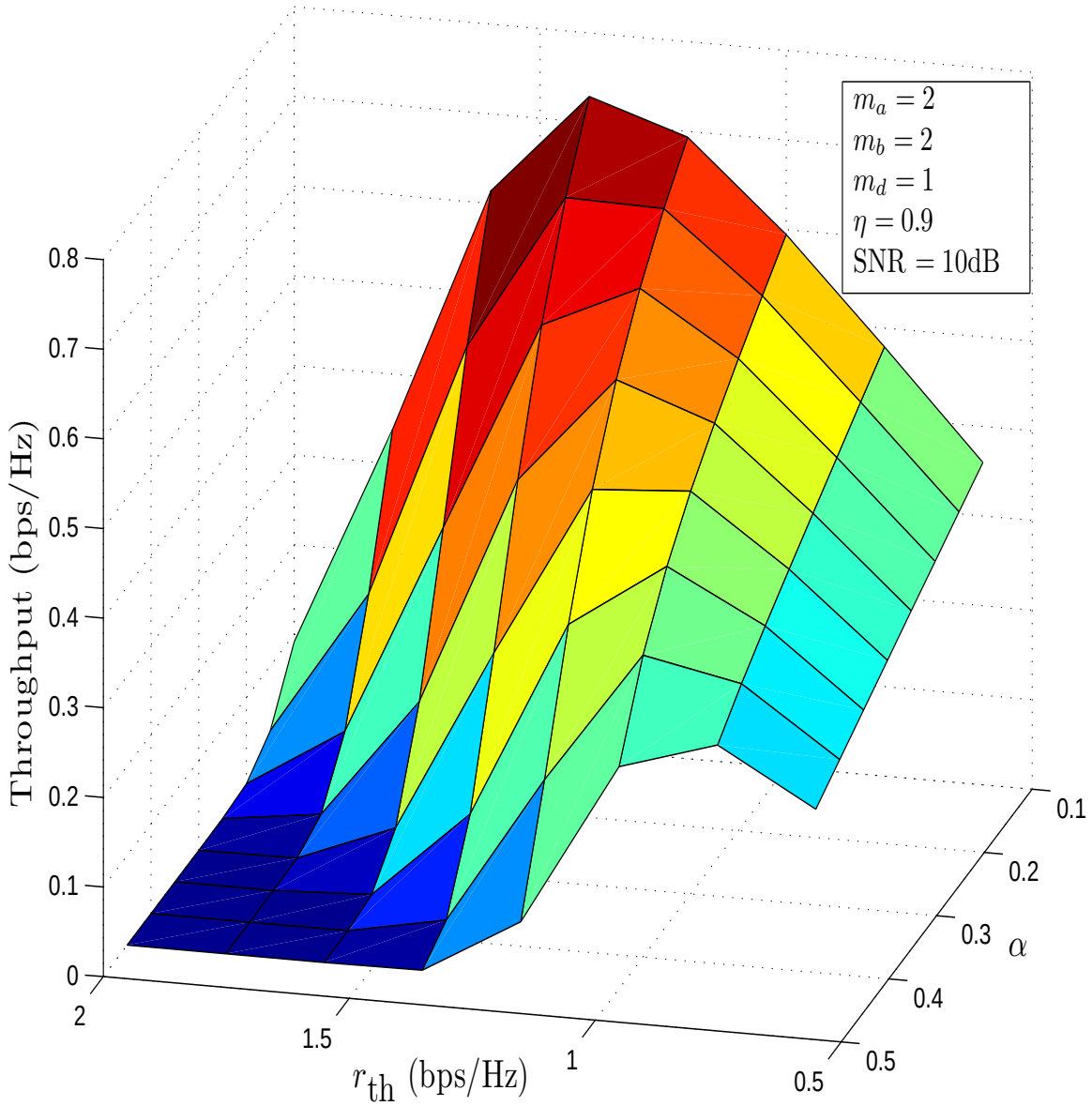

Figure 5.4: Joint effect of r_{th} and α on the system throughput.

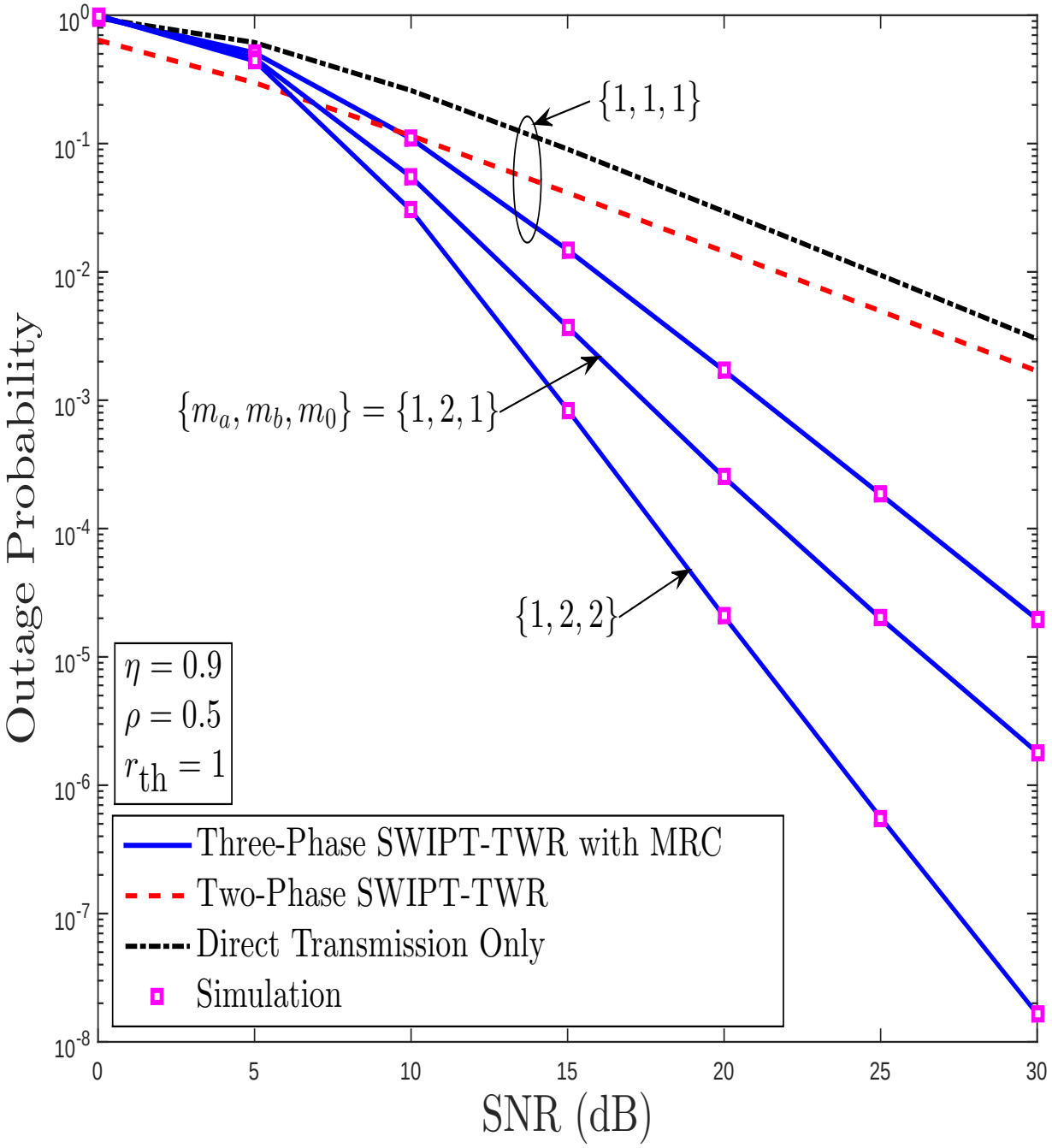

Figure 5.5: OP versus SNR curves of link $S_b \to S_a$.

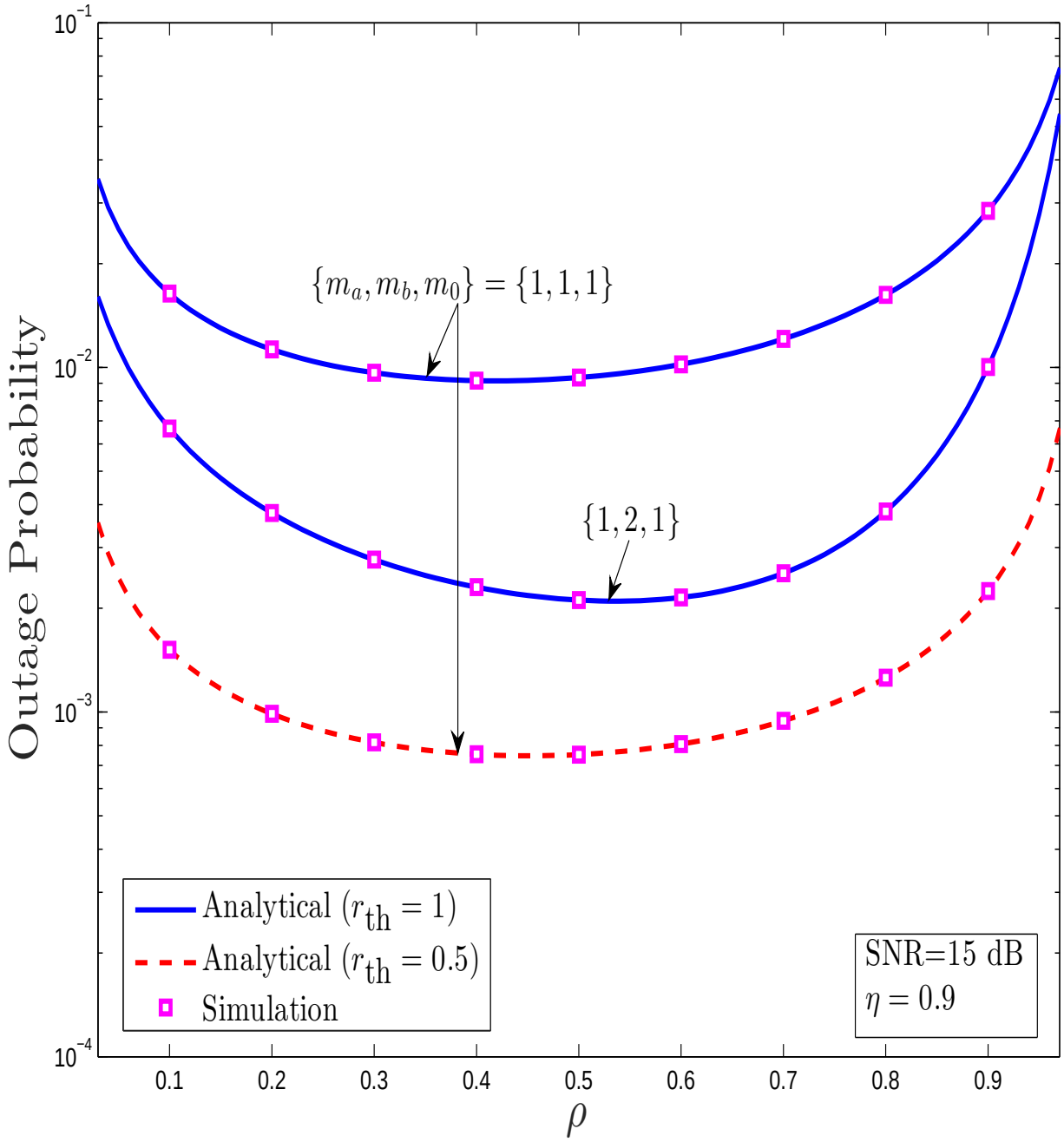

Figure 5.6: OP versus ρ curves of link $S_b \to S_a$.

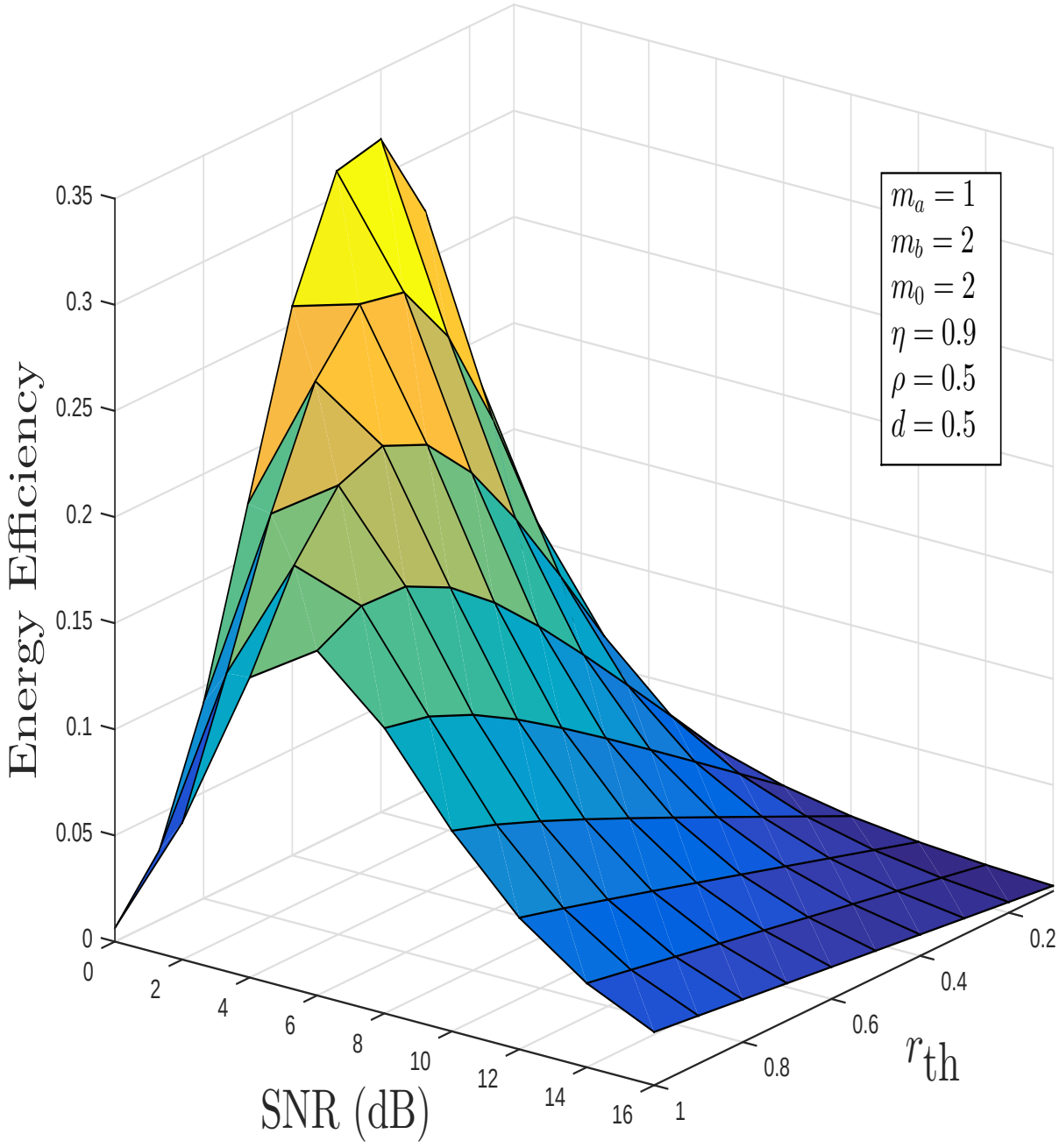

Figure 5.7: Energy efficiency versus SNR and r_{th}.

Chapter 6

Conclusion and Future Works

In this chapter, we conclude our work and provide the possible future scope for it.

6.1 Conclusion

In this thesis, bidirectional hybrid and AF based TWR networks have been considered, where an energy assisted relay node harvests energy from the received RF signal. We considered two EH approaches viz., TS and PS to enable EH and IP at the relay.

Firstly, we investigated the performance of TS-enabled TWR system where a hybrid relaying scheme is adopted at the relay node. We analyzed the outage performance of the considered system by deriving the expressions of OP and system throughput for SC diversity combining scheme at the destination nodes under Nakagami-m fading channels. Numerical and simulation results elucidated the significance of adopting HDAF relaying scheme whereby it was shown that our considered scheme outperforms the other similar schemes such as SWIPT-AF and SWIPT-DF in terms of OP and system throughput.

Secondly, we examined the performance of PS-enabled three phase TWR system where an AF relaying scheme is adopted at the relay node and MRC adopted at the destination node. We first derived the OP expression of the considered system under Nakagami-m fading channels. Then, we obtained the expressions of system throughput and energy efficiency. Numerical and simulation results elucidated the significance of

SWIPT with exploitation of a direct link in TWR networks.

6.2 Future Works

In this section, we summarize the future research scopes of our work.

- For the considered system, performance analysis can be done by applying hybrid energy supplies via both EH from RE sources and RF signals. We can utilize the offline and online energy management schemes in EH from the RE sources for communication networks.

- In this system, we will replace the half-duplex relaying by the full-duplex relaying scheme. Also, we will consider co-channel interference at the relay node which can be used to harvest more energy from the RF signals. We will integrate the TS and PS schemes in a single receiver antenna which is called as hybrid relaying protocol.

- We will use the concept of EH in future cognitive radio networks, where secondary users can harvest the energy from the primary users through RF and RE sources. For OP minimization, we can employ linear optimization algorithms to optimize the TS and PS factors under the constraint of fairness system throughput and transmitted power.

- We will utilize the SWIPT technique in future OFDM systems, where PS is performed before digital OFDM demodulation. Thus, all sub-carriers would have the same PS ratio at each receiver.

REFERENCES

[1] M. Etoh, T. Ohya, and Y. Nakayama, "Energy consumption issues on mobile network systems," in *Proc. Int. Symp. on Appl. Inter.*, 2008.

[2] M. Zorzi, A. Gluhak, S. Lange, and A. Bassi, "From todays INTRAnet of things to a future INTERnet of things: A wireless and mobility-related view," *IEEE Wireless Commun.*, vol. 17, no. 6, pp. 1536-1284, Dec. 2010.

[3] J. Zhou, M. Li, L. Liu, X. She, and L. Chen, "Energy source aware target cell selection and coverage optimization for power saving in cellular networks," in *Proc. IEEE/ACM Int. Conf. Green Comput. Commun., Int. Conf. Cyber, Physical Social Comput.*, Dec 2010.

[4] V. Raghunathan, S. Ganeriwal, and M. Srivastava, "Emerging techniques for long lived wireless sensor networks," *IEEE Commun. Mag.*, vol. 44, no. 4, pp. 108-114, Apr. 2006.

[5] C. Peng, F. Li, and H. Liu, "Optimal power splitting in two-way decode-and-forward relay networks," *IEEE Commun. Lett.*, vol. 21, no. 9, pp. 2009-2012, Sep. 2017.

[6] R. Zhang and C. K. Ho, "MIMO broadcasting for simultaneous wireless information and power transfer," *IEEE Trans. Wireless Commun.*, vol. 12, no. 5, pp. 1989-2001, May 2013.

[7] H. Lee, K.-J. Lee, H. Kim, B. Clerckx, and I. Lee, "Resource allocation techniques for wireless powered communication networks with energy storage constraint," *IEEE Trans. Wireless Commun.*, vol. 15, no. 4, pp. 2619-2628, Apr. 2016.

[8] L. R. Varshney, "Transporting information and energy simultaneously," in *Proc. IEEE ISIT*, pp. 1612-1616, July 2008.

[9] J. N. Laneman, D. N. C. Tse, and G. W. Wornell, "Cooperative diversity in wireless networks: Efficient protocols and outage behavior," *IEEE Trans. Inf. Theory*, vol. 50, no. 12, pp. 3062-3080, Dec. 2004.

[10] X. Zhou, R. Zhang, and C. K. Ho, "Wireless information and power transfer: Architecture design and rate-energy tradeoff," *IEEE Trans. Commun.*, vol. 61, no. 11, pp. 4754-4767, Nov. 2013.

[11] A. A. Nasir, X. Zhou, S. Durrani, and R. A. Kennedy, "Wireless-powered relays in cooperative communications: Time-switching relaying protocols and throughput analysis," *IEEE Trans. Commun.*, vol. 63, no. 5, pp. 1607-1622, May 2015.

[12] I. Krikidis, S. Timotheou, and S. Sasaki, "RF energy transfer for cooperative networks: Data relaying or energy harvesting," *IEEE Commun.Lett.*, vol. 16, no. 11, pp. 1772-1775, Nov. 2012.

[13] J. Men, J. Ge, C. Zhang, and J. Li, "Joint optimal power allocation and relay selection scheme in energy harvesting asymmetric two-way relaying system," *IET Commun.*, vol. 9, no. 11, pp. 1421-1426, July 2015.

[14] B. Rankov and A. Wittneben, "Spectral efficient protocols for half-duplex relay channels," *IEEE J. Sel. Areas Commun.*, vol. 25, no. 2, pp. 379-389, Feb. 2007.

[15] P. K. Upadhyay and S. Prakriya, "Performance of two-way opportunistic relaying with analog network coding over Nakagami-m fading," *IEEE Trans. Veh. Technol.*, vol. 60, no. 4, pp. 1965-1971, May 2011.

[16] S. Yadav and P. K. Upadhyay, "Performance of three-phase analog network coding with relay selection in Nakagami-m fading," *IEEE Commun. Lett.*, vol. 17, no. 8, pp. 1620-1623, Aug. 2013.

[17] M. Ju and I.-M. Kim, "Relay selection with ANC and TDBC protocols in bidirectional relay networks," *IEEE Trans. Commun.*, vol. 58, no. 12, pp. 914-916, Dec. 2010.

[18] G. Du, K. Xiong, Y. Zhang, and Z. Qiu, "Outage analysis and optimization for time switching-based two-way relaying with energy harvesting relay node," *KSII Trans. Internet and Info. Systems*, vol. 9, no. 2, pp. 545-563, Feb. 2015.

[19] T. Li, P. Fan, and K. B. Letaief, "Outage probability of energy harvesting relay-aided cooperative networks over rayleigh fading channel," *IEEE Trans. Veh. Techn.*, vol. 65, pp. 972-978, Jan. 2016.

[20] J. Men, J. Ge, C. Zhang, and J. Li, "Joint optimal power allocation and relay selection scheme in energy harvesting asymmetric two-way relaying system," *IET Commun.*, vol. 9, no. 11, pp. 1421-1426, July 2015.

[21] G. Du, K. Xiong, Y. Zhang, and Z. Qiu, "Outage analysis and optimization for time switching-based two-way relaying with energy harvesting relay node," *KSII Trans. Internet and Info. Systems*, vol. 9, no. 2, pp. 545-563, Feb. 2015.

[22] R. Hu and T.-M. Lok, "Power splitting and relay optimization for two-way relay SWIPT systems," in *Proc. IEEE ICC*, Malaysia, May 2016.

[23] T. P. Do, I. Song, and Y. H. Kim, "Simultaneous wireless transfer of power and information in a decode-and-forward two-way relaying network," *IEEE Trans. Wireless Commun.*, vol. 16, no. 3, pp. 1579-1592, Mar. 2017.

[24] R. Hu and T.-M. Lok, "Power splitting and relay optimization for two-way relay SWIPT systems," in *Proc. IEEE ICC*, Malaysia, May 2016.

[25] Y. Liu, L. Wang, M. Elkashlan, T. Q. Duong, and A. Nallanathan, "Two-way relay networks with wireless power transfer: Design and performance analysis," *IET Commun.*, vol. 10, no. 14, pp. 1810-1819, June 2016.

[26] N. T. P. Van, S. F. Hasan, X. Gui, S. Mukhopadhyay, and H. Tran, "Three-step two-way decode and forward relay with energy harvesting," *IEEE Commun. Lett.*, vol. 21, no. 4, pp. 857-860, Apr. 2017.

[27] C. Peng, F. Li, and H. Liu, "Optimal power splitting in two-way decode-and-forward relay networks," *IEEE Commun. Lett.*, vol. 21, no. 9, pp. 2009-2012, Sep. 2017.

[28] T. P. Do, I. Song, and Y. H. Kim, "Simultaneous wireless transfer of power and information in a decode-and-forward two-way relaying network," *IEEE Trans. Wireless Commun.*, vol. 16, no. 3, pp. 1579-1592, Mar. 2017.

[29] L. Liu, R. Zhang, and K. C. Chau, "Wireless information transfer with opportunistic energy harvesting," *IEEE Trans. Wireless Commun.,* vol. 12, no. 1, pp. 288-300, Mar. 2013.

[30] X. Zhou, "Traning-based SWIPT: Optimal power splitting at the receiver," *IEEE Trans. Veh. Tech.*, vol. 64, no. 9, pp. 4377-4382, Sept. 2015.

[31] A. F. M. Shahen Shah, Md. Shariful Islam, "A survey on cooperative communication in wireless networks," *I.J. Intelligent Systems and Applications.*, vol. 64, no. 9, June 2014

[32] Z. Popovic, "Cut the cord: Low-power far-field wireless powering," *IEEE Microw. Mag.*, vol. 14, no. 2, pp. 55-62, Mar. 2013.

[33] N. C. Beaulieu and C. Cheng, "Efficient Nakagami-m fading channel simulation," *IEEE Trans. on Veh. Tech.*, vol. 54, no. 2, Mar. 2005.

[34] I. Gradshteyn and I. Ryzhik, "Table of integrals, series, and products," *Academic Press, San Diego, California,* 7th ed., 2007.